2018-01-01

An Integrated Study Towards Curing Neurodegenerative Disorders Using Materials Science And Stem Cell-Based Tissue Engineering Approaches

Nishat Tasnim
University of Texas at El Paso, tasnim.nishat2@gmail.com

AN INTEGRATED STUDY TOWARDS CURING NEURODEGENERATIVE DISORDERS USING MATERIALS SCIENCE AND STEM CELL-BASED TISSUE ENGINEERING APPROACHES

NISHAT TASNIM

Doctoral Program in Materials Science and Engineering

APPROVED:

Binata Joddar, Ph.D., Chair

Devesh Misra, Ph.D.

David Roberson, Ph.D.

Guikuan Yue, Ph.D.

Munmun Chattopadhyay, Ph.D.

Charles Ambler, Ph.D.
Dean of the Graduate School

Dedication

I would like to dedicate this dissertation to my parents and sister for their inspiration, my parents-in-law for their support and to my husband for always being by my side.

AN INTEGRATED STUDY TOWARDS CURING NEURODEGENERATIVE DISORDERS USING MATERIALS SCIENCE AND STEM CELL-BASED TISSUE ENGINEERING APPROACHES

by

NISHAT TASNIM, M.S in Electrical Engineering

DISSERTATION

Presented to the Faculty of the Graduate School at

The University of Texas at El Paso

in Partial Fulfillment

of the Requirements

for the Degree of

DOCTOR OF PHILOSOPHY

Department of Metallurgical, Materials and Biomedical Engineering

THE UNIVERSITY OF TEXAS AT EL PASO

May 2018

Acknowledgements

At first, all praise and worthiness go to Almighty Merciful Allah for giving me the opportunity and ability to see my endeavor in becoming successful. I want to express my profound gratitude to my Ph.D. supervisor, Dr. Binata Joddar, for her tremendous guidance, kind encouragement, sympathetic co-operation, and invaluable suggestion that helped me to accomplish my doctoral research. Her continuous assessment and mentoring throughout my doctoral studies made me a better engineer and researcher.

I would like to thank my dissertation committee members, Dr. Munmun Chattopadhyay for her kind inputs in confocal microscopy imaging, Dr. David Roberson for his generous assistance in scanning electron microscopy imaging, Dr. Devesh Misra for his sincere guidance and Dr. Guikuan Yue for his thoughtful feedbacks. I am extremely thankful to Vikram Thakur for his kind assistance and valuable time given to me in some of my key experiments. I appreciate the assistance of all the past and present members of my research group from Inspired Materials and Stem Cell-based Tissue Engineering Laboratory (IMSTEL) and our collaborators who helped me to achieve my research goals. I am grateful to the funding sources, facilities and the undoubted support of the faculty, staff and students in the department of Metallurgical, Materials and Biomedical Engineering at the University of Texas at El Paso.

I am thankful to my family and friends for their blessings, encouragements and constant support which provided me with the confidence and enthusiasm to successfully complete my graduate studies. Finally, my special thanks go to my beloved husband, Ridwan Fayaz Hossain, for not only being my strength and courage but also for helping me in certain aspects of my research.

Abstract

Neurodegenerative diseases affect around one billion people globally that are characterized by irreversible degeneration of brain tissues. These diseases cause serious effects on patients degrading their brain functions and causing enormous physical and mental health issues. Parkinson's disease (PD) is one of the most common neurodegenerative disorder affecting millions of people worldwide which results from loss of dopaminergic (DA) neurons in the mid-brain. Unfortunately, no medical treatment is effective to date for these significant brain disorders, except some symptomatic therapies only focusing on improving the quality of patient's life.

Two current approaches hold great promise in targeting PD as well as other neurodegenerative diseases, by surgically implanting electrodes for deep brain stimulation (DBS) and transplanting healthy neuronal cells at the site of tissue loss, due to disease in the brain. However, cells for transplantation need to be delivered via a scaffold. Nerve regeneration in a scaffold of appropriate biomaterial is of great importance while being implanted inside the animal body for further clinical applications. In this dissertation, both approaches for treating PD were incorporated by in vitro studies using surface-engineering and tissue-engineering techniques. For the first approach, graphene oxide (GO) coatings on commercially available 316L stainless steel (SS) surfaces was done to reduce the neurotoxicity of SS and modified surfaces showed hydrophilicity, biocompatibility, cell proliferation, and decreased reactive oxygen species (ROS) expression with SHSY-5Y neuroblastoma cell lines.

Transplantation of stem cells in vivo is another approach for reducing the progression of PD by reversing the loss of affected DA neurons. So, our second approach included differentiation of mesenchymal stem cells into DA neurons using Sonic hedgehog, Fibroblast growth factor, Basic fibroblast growth factor and Brain-derived neurotrophic factor, while they were cultured within collagen coated three-dimensional (3D) Graphene foams. 3D multilayer graphene scaffold could mimic the actual brain tissue environment and more closely exhibit morphologies, functions and other necessary characteristics compared to 2D culture on tissue culture plastic. The graphene-

based scaffolds were not cytotoxic as cells seemed to retain viability and proliferated substantially during in vitro culture. These results suggest the utility of Graphene-based materials towards neuronal and stem cell culture, which is an important step for neural tissue engineering applications.

Table of Contents

List of Tables

List of Figures

Chapter 1: Introduction

Among all organs in our body, brain is the most complex containing billions of nerve cells and fibers that are in turn connected by trillions of connections called synapses [1]. The brain is anatomically divided into specialized areas which work together to receive inputs from the sensory organs and send outputs to the muscle tissues. It controls all the voluntary and involuntary functions of the body. Any condition that affects this complex anatomy can result in chronic conditions such as those observed in neurodegenerative disorders including Parkinson's disease (PD), Alzheimer's (AZ) and Amyotrophic Lateral Sclerosis (ALS), which can affect our movement and thinking abilities.

Nervous system consists of two main parts, central nervous system (CNS) and peripheral nervous system (PNS). The CNS consists of brain and spinal cord which controls most functions of the body and mind, while the PNS includes all the other parts of the nervous system except brain and spinal cord. The CNS serves the purpose of communication, homeostasis and mental activity. Nerve tissue, the primary tissue of the central nervous system consisting of many cells including neurons and glial cell regulates the bodily activities. Neurons are electrically excitable cells and primary component of the central nervous system that transmit and receive messages through electrical and chemical signals via synapses in a neural network. Degeneration or death of neuronal cells leads to neurodegenerative disorders which constitutes the greater portion of neurological diseases. These types of diseases include AZ, PD, ALS, and Huntington's disease, most of the time caused by genetic mutations, environmental health problems, aging, brain injury and some intracellular mechanisms [2]. Current treatment for neurological disorders includes variety of medications and treatments, physical therapies and sometimes even surgical interventions, all of which cannot stop the breakdown of neuronal cells and as a result cannot restore the normal brain functions of the patient [3]. The most common medicines- carbidopa, levodopa and dopamine agonists can control some symptoms of PD, but have lots of side effects including dizziness, restlessness, headache, nausea, stomach pain, and low blood pressure. Furthermore, medicines for

PD can only control the motor symptoms [4]. Deep brain stimulation (DBS) surgery with implantable electrodes is another treatment used to treat more advanced cases and offer symptomatic treatment of PD, especially in those where the drugs are not effective to improve the condition of the patients. DBS surgery reduces the symptoms like bradykinesia and rigidity but not tremor [5]. So even after the surgery, the patients need to depend on the medications for some of the motor symptoms.

Neurological disorders have significant impacts on the world's economy and represent a large portion of global burden of disease [6, 7]. According to ITIF (Information technology and Innovation foundation), brain disorders cost the U.S. economy more than $1.5 trillion per year. Hence, now researchers are investigating how tissue engineering and regenerative medicine could be used to find innovative ways to treat or prevent the brain diseases in a more economically feasible way.

1.1 Background

Parkinson's disease (PD) is increasingly being identified as a highly complex neurodegenerative disorder with complications arising from co-occurring pathologies and diverse contributing risk factors, such as ageing, genetics and environmental toxins. The disease is considered as the second most common neurodegenerative disorder encapsulated by the loss of midbrain dopaminergic (DA) neurons in the substantia nigra pars compacta (SNPC) (Figure 1.1) affecting mostly the aged people as well as young adults. [8, 9]. About 10%-20% of those diagnosed with Parkinson's disease are under age 50, and about half of those are diagnosed before age 40 [10]. Approximately 60,000 new cases of Parkinson's are diagnosed each year in the United States, meaning somewhere around 6,000 – 12,000 are young onset patients [11]. Thus, PD has been extremely important to diagnose and treat at an early onset compared to later and more advanced stages of the disease in affected individuals.

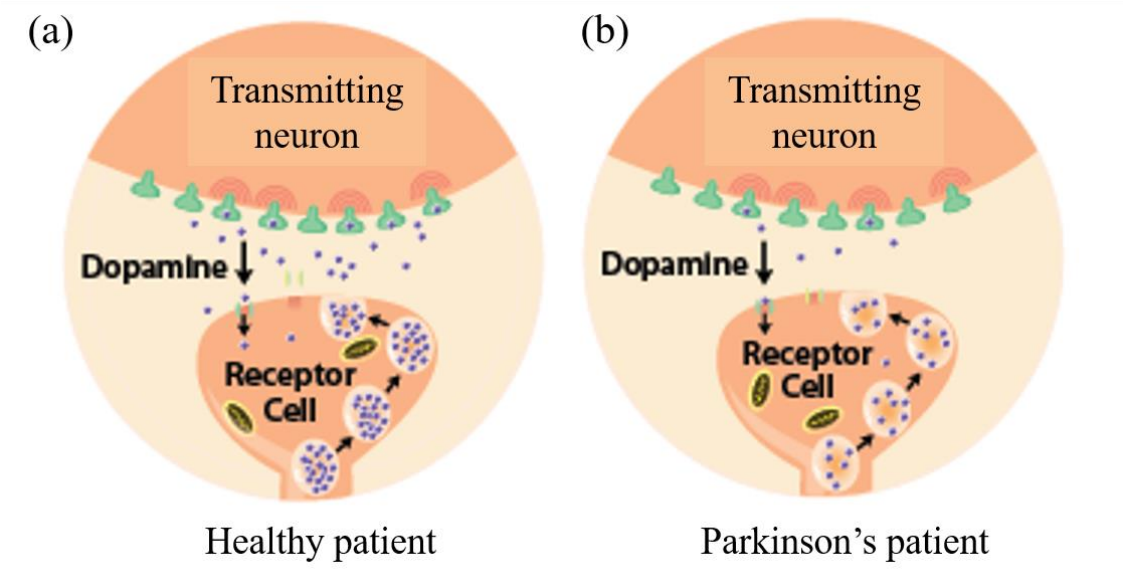

Figure 1.1: Parkinson's patients have less dopamine, shown in (a) healthy patients have more dopamine producing neurons and (b) Parkinson's patient's dopamine producing cells are damaged or dead [adopted from NIH website]

Micronutrient deficiency has remarkable effects on neural tissue functions. There are certain micronutrients, usually some vitamins and minerals, that can prevent the onset of Parkinson's disease as well as other neurodegenerative disorders in youth, such as magnesium, folic acid, zinc and so on [12, 13]. Many of the non-motor symptoms like dementia and dysphagia can be prevented by intaking vitamins or phytonutrients. In PD, non-motor symptoms might be responsible for the impairment of fluid and micronutrient balance, and pharmaconutrient interactions [14]. Zinc performs important functions in the early development and maintenance of the brain in a fetus. A fetus in a pregnant women being low in Zn and high in Cu may later manifest themselves as schizophrenia, autism or epilepsy as well as corresponding increase in oxidative damage, eventually leading to PD [15]. Therefore, efforts must be directed to prevent the onset and progression of PD by controlling the diet, nutrition, and nutrients along with environmental

risk factors by the side of current treatment which is mainly focused on symptomatic management [16].

The loss of DA neurons occurs with formation of Lewy bodies and lewy neurites, which are mainly formed by insoluble aggregates of α -synuclein (coded by SCNA). A large number of motor and non-motor features including muscle rigidity, resting tremors, bradykinesia, depression, cognitive dysfunction, and sleep disorders appear when 60–80 % of dopamine (DA) neurons are degenerated causing the neurochemical changes in the striatum due to loss of nigrostriatal axon terminals [17, 18]. In most of the cases, PD is sporadic having different pathologies, instead of being familial PD (fPD), which suggest that the genetic factors play a minor role in causing typical PD [19]. Patients with autosomal-dominant fPD typically show extensive formation of Lewy bodies in different parts of the brain unlike patients with autosomal-recessive fPD [20]. Mutations of the proteins SNCA, LRRK2, PARK2, PINK1, and PARK7 possess important roles in the pathogenesis of the disease among which SNCA and LRRK2 are leading to the autosomal-dominant forms of the disease [21]. Lewy bodies composed of α-synuclein encoded by SNCA gene aggregate in both inherited and sporadic forms of the disease [22]. Ten different subtypes of DA neurons have been identified in the whole brain among which A8, A9, and A10 reside in the midbrain [23]. The loss of the pigmented A9 DA neurons of the ventrolateral pars compacta which control movement gives rise to the symptoms of PD [24]. Non-motor symptoms like olfactory dysfunction, sleep disturbance, dementia and smell loss are caused by the aggregation of α -synuclein forming Lewy bodies in various parts of the brain of a PD patient. The spread of α -synuclein corresponding to the worsening of Symptoms in Parkinson's is shown in Figure 1.2 [25].

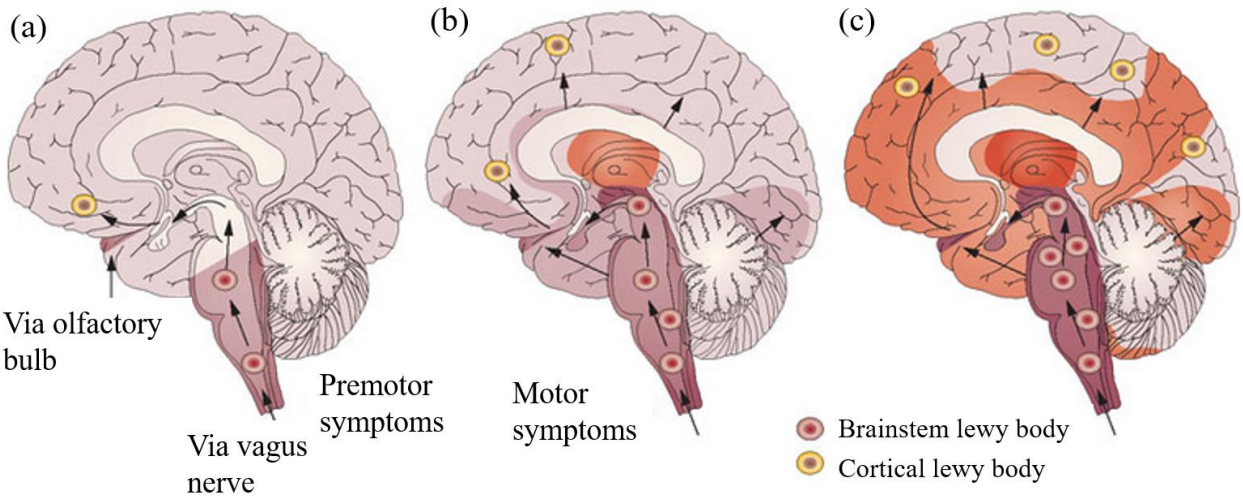

Figure 1.2: Spread of α -synuclein corresponding to the worsening of Symptoms in Parkinson's is shown in (a) autonomic and olfactory disturbances, (b) sleep and motor disturbances and (c) emotional and cognitive disturbances.

Though existing treatments for PD including dopamine replacement drugs such as levodopa, carbidopa and deep brain stimulation (DBS) are effective in improving the symptoms of the patients, they are not able to stop PD progression [26, 27].

DBS is an established open-brain-surgery treatment for PD which involves implantation of neural electrodes which sends electrical impulses to the specific targets in the brain for deep brain recording. Besides, neural implants have significant role in understanding the disease pathology. In vivo recording of neural activity by brain electrodes contains the risk of scar tissue formation in case of functional brain signal recording. The scar tissue encapsulates the electrode, creating a physical barrier between the electrode surface and the brain. Thus, the electrode–brain interface of these devices needs to withstand the challenge of chronic recording with minimal effect on the surrounding tissue [28]. Hence, modifying the surface of the electrode by biomolecule immobilization applying surface engineering techniques enhances the overall biocompatibility and

efficacy of the electrodes [29]. Several coating materials have been used to reduce the level of scarring and enhancing the biocompatibility of the electrodes for deeper brain sites, including diamond-like carbon [30], SiC [31], TiN [32], TiO_2 [33], polymers [34] and biological moieties such as heparin [35] and dopamine [36] are usually adopted for a variety of applications. Each of these coating materials have inherent limitations of instability. Specifically for neural implant electrodes iridium oxide coatings [37], multiwalled carbon nanotubes (MWNTs) and gold coatings [38] [39] and a conductive polymer coating has been shown to improve the electrochemical properties of electrodes [40]. However, all implantable electrodes in Chronic Neural Interfaces (CNI) encounters a common problem of deteriorating in performance of recording capabilities over time because of tissue injury and adverse reactions with the coating materials of the implants [41]. To solve this issue, novel inert materials need to be explored as coating materials for neural electrodes.

A molecular-level road-mapping of PD progress is challenged by the lack of access to affected human DA neurons along the disease trajectory. Besides, animal studies designed to provide an advanced prototype of PD often suffer from differing vulnerabilities to disease-causing factors. Therefore, stressors or genetic risk factors, which play an important role in the pathogenesis of PD in humans, may not be revealed by animal studies. As studying neuronal cell death in human brains is extremely difficult and invasive, development of in-vitro models of DA neurons would make it possible to understand cellular and molecular mechanisms of the neurodegenerative disorders and novel therapeutic strategies [42]. Different cellular models have been established to investigate the mechanisms underlying PD [43]. Current models for studying PD rely on neuronal cell lines such as SHSY-5Y, N27, N2a and PC-12 as a means to define disease causals and progress. However, these cell types neither satisfactorily reproduces cardinal features

associated with the disease nor facilitate drug screening efforts against PD. As a result, discoveries arising from such cellular models, which are usually not based on human DA neurons, may not fully reflect true disease pathogenesis and pathology that would otherwise likely be observed in DA neurons [44].

Recently several researchers are trying to replace lost DA neurons using stem cells such as neural stem cells (NSCs), embryonic stem cells (ESCs), mesenchymal stem cells (MSCs), and induced pluripotent stem cells (iPSCs). Human induced pluripotent stem cell (iPSC) and human Mesenchymal Cell (MSC) lines are particularly advantageous to study PD progression and may fill the gap in aforementioned PD models. For example, iPSC lines generated from idiopathic patients lacking known PD mutations offer the opportunity to investigate the degree to which patient cells are inherently dysfunctional (due to the contribution from background genetic susceptibility). A second potential advantage in iPSC-derived cultures is that they facilitate in vitro clinical trials, whereby the genetic diversity seen in populations can be captured in vitro. This permits the investigation of genotype-dependent drug efficacies. MSC have advanced in their applications to form diverse tissue types and possess the potential to treat a wide range of acute and degenerative diseases making them particularly attractive to PD studies and treatment.

1.2 Rationale and Hypotheses

Parkinson's disease (PD) is a debilitating neurodegenerative disorder characterized by progressive slowness of movement and loss of the brain chemical dopamine, with no known cure. Molecular level investigations have revealed the accumulation and aggregation of toxic proteins/biomarkers such as α-synuclein and synphilin-1 in DA neurons affected by PD. Current treatment options for PD includes implantation of electrodes for DBS. However, all implantable electrodes encounter a common problem of deterioration in performance of recording capabilities over time because of tissue injury and adverse reactions. Therefore, studies must be done to

understand the modulation and disease progression of PD in cell culture models in vitro, to devise therapeutic strategies to inhibit the progression of PD.

Stainless steel (SS) alloys are often used as biomedical implants with applications in cardiovascular, orthopaedic and dentistry due to their superior mechanical properties. However the neurotoxicity of iron present in stainless steel makes it unsuitable as neuronal implants [45]. The use of inert materials is of special importance for neural electrodes used for DBS, useful in a therapy of movement disorders including PD [46]. Acute misbalance of brain iron homeostasis has been linked to acute neuronal injury following cerebral ischemia [47]. Free iron is known to catalyse the conversion of superoxide and hydrogen peroxide into hydroxyl radicals, which generate oxidative stress leading to subsequent apoptosis of neurons [47]. Besides, bare metallic SS surfaces are often affected by biological corrosion in vivo [46], and etching releasing sub-lethal concentrations of metallic ions which could exacerbate the pro-inflammatory and fibrotic reactions [47, 48]. Surface modification plays an effective role to alleviate these adverse physiological responses to the SS implants. Studies have shown that graphene oxide (GO) films allowed the effective proliferation of human and mammalian cells with limited or no cytotoxicity [49, 50]. Specifically, GO has been recently shown to promote the growth of neuronal cells [49, 51], human osteoblasts [52] and even promoted osteogenic differentiation of human mesenchymal stem cells [53]. In one of our previous study, GO-coated surfaces significantly enhanced endothelial cell adhesion, proliferation and reduced ROS expression compared with bare implant surfacese. Such characteristics seem to indicate that GO may be an ideal candidate for coating implant surfaces along with the fact that GO is also chemically inert, electrically-conductive and durable [54-56]. These reports motivated us to further explore the feasibility of coating bare 316L SS surfaces with GO, and to determine the ability of these GO-coatings in enhancing the biocompatibility of existing 316L SS implant surfaces. In addition GO-coatings adhere strongly to underlying surfaces thereby forming an over–coating and a protective layer at the same time [57]. GO can be applied as surface coatings of electrodes currently used in DBS used to treat PD patients. ***We hypothesized that GO coated SS surfaces will have optimized properties for application as neural implants,***

will promote neural outgrowth and reduce the progression of degenerative pathologies in diseased PD neurons. Further we believe this technique of GO-coating could be applied to other metallic implant surfaces wherever the development of such protective coatings is necessary.

Another therapeutic approach for PD is cell replacement therapy (CRT), a restorative therapy designed to secure a long-lasting relief of patients' symptoms. Cell based replacement therapy utilizing stem cells holds immense potential as a long-term treatment for PD. MSC can serve in stem-cell-replacement-therapy which is a powerful tool for investigating disease pathology and for advancing clinical therapies. To make feasible, studies involving the role of material interactions with human DA neurons in a dish, we differentiated human mesenchymal stem cells (MSC) into DA neurons [58]. Using these human stem cell differentiated DA neuron-PD transfected cell culture models, we aimed to study interactions between DA neurons and three-dimensional (3D) graphene foam (GF) that will reduce or mitigate the progression of PD in-vitro. On the basis of strong preliminary data [59], ***we hypothesized that culture atop nanotextured Graphene-based substrates will be extremely effective in reducing the progression of PD pathogenesis in human MSC differentiated DA neuron-PD transfected cells. The novelty of this study is based on the hypothesis that differentiating mesenchymal stem cells in a three-dimensional (3D) scaffold into DA neurons can be used for cell transplantation therapy for the treatment of Parkinson's disease.***

1.3 Objectives

The objective of this research project was to develop biocompatible and adherent thin film coated SS electrodes for use in DBS therapy as a potential alternative to high cost Platinum (Pt) electrodes for treatment of PD in affected population. We aimed to develop a novel coating utilizing GO to surface-modify existing SS surfaces to enhance their biocompatibility and functional uniqueness. We are interested in using less-toxic polymer-free materials which will confer biocompatibility and conductivity for SS implant surfaces. The first aim of this study was to develop a GO-coating for surface modification of existing SS implant surfaces, to assess and

characterize the material properties, resistance to degradation and unique functionalities including conferring of GO-coatings and to assess the biocompatibility of the GO-coated SS implants by in-vitro cell culture experiments.

In contrast, stem cells can be differentiated to grow dopamine-producing DA neurons in vitro, enabling studies exploring the genetic basis for such diseases on a dish in vitro. Further, CRT using stem cells is considered as a potential approach to treat PD, given that the progressive neuronal loss of DA neurons characterizes them. Human iPSCs reprogrammed from adult human somatic cells; and human MSCs from the bone-marrow or adipose represent a promising unlimited cell source for generating patient-specific cells for biomedical research and personalized medicine. The second aim of the study was to differentiate DA neurons from MSC. This MSC differentiated DA neuron-PD induced cell culture model will become a powerful tool and enable modeling and treatment of PD in a dish in vitro. In addition to revealing the mechanisms involved in modulating the disease progression in PD, our future studies will test the ability of potential novel material interventions to restore or reduce the level of PD in affected DA neurons. Accordingly, the study was executed.

Specific Aim 1: To develop a GO-coating for surface modification of existing SS implant surfaces characterizing the material properties and testing biocompatibility of the GO-coated SS implants by in-vitro cell culture experiments.

Specific Aim 2: To test the efficacy of 3D multilayer Graphene-based scaffolds towards the adhesion, proliferation and maintenance of neuronal-phenotype by MSC differentiated DA neurons scaffolds in reducing the progression of PD pathogenesis in MSC differentiated DA neurons.

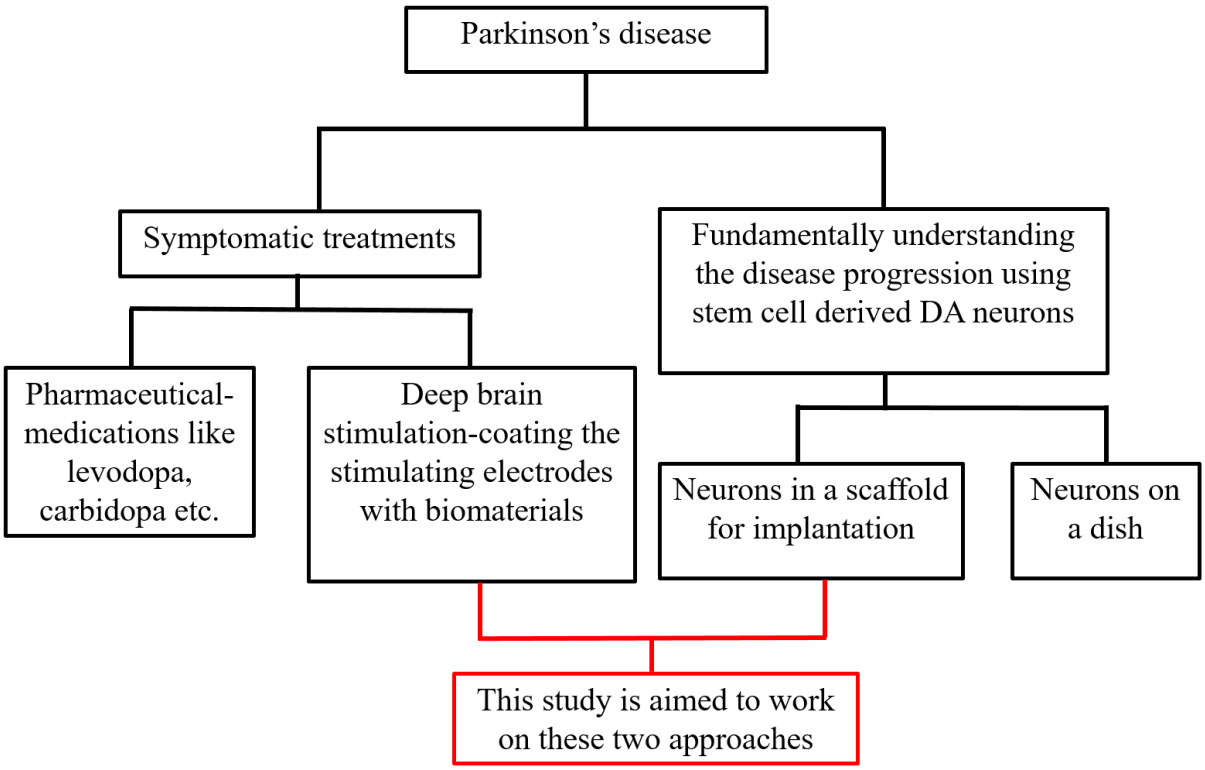

Figure 1.3: The objective of this study is to reduce Parkinson's disease progression by surface modification and differentiating dopaminergic neurons from mesenchymal stem cells.

In Figure 1.3, the two potential therapeutic approaches for PD is shown as symptomatic treatments and fundamentally understanding the disease progression using stem cell derived DA neurons. The objective of this study aimed in both approaches by coating electrodes for DBS by novel biomaterial and differentiating DA neurons in a scaffold for implantation. In the first study, our objective was to utilize a commercially available 3D biocompatible scaffold made of GF for culturing MSC and differentiating into DA neurons. Our hypothesis was that differentiated DA neurons when cultured in a 3D hydrogel-based scaffold at a high density, will more closely exhibit morphologies, functions and other necessary characteristics compared to 2D culture on tissue culture plastic. However, as the GF is extremely hydrophobic, to make it hydrophilic collagen gel was used as a coating material which is hydrophilic but lacks mechanical stability and electrical conductivity, whereas GF is hydrophobic but electrically conductive [60]. So, to combine and

extract the best of both materials, collagen was deposited over the GF and crosslinked using genipin [61], which a hydrophilic, porous yet conductive scaffold ideal for neuron culture.

This work will significantly contribute by allowing us to study interactions between healthy DA neurons, their synapses and communications, and predict mechanisms involved in DA neuron apoptosis during injury and disease. As studying neuronal cell death in human brains is extremely difficult and invasive, development of *in vitro* models of DA neurons would make it possible to understand cellular and molecular mechanisms of the neurodegenerative disorders and novel therapeutic strategies. This study is innovative as the 3D tissues will facilitate investigation of human DA neuronal function and disease and may be adaptable for engineering other 3D tissues from different stem cell types. The interactions between DA neurons (including healthy and PD induced state) and Graphene-based substrates can lead to material-based approaches for treatment of not only PD but will undoubtedly also be useful to other research groups and impact other synucleinopathies such as Huntington's, ALS and Alzheimer's.

In the second study, MSC was differentiated into DA neurons using established protocols [58], and characterized using antibodies for β-III tubulin, tyrosine hydroxylase and their dopamine secretion. For this differentiation process, MSC was seeded atop 3D GF scaffold and then induced for differentiation. The extent of cell adhesion, proliferation and maintenance of DA neuron morphology of cells grown on Graphene-based substrates was observed, quantified and compared to DA neurons passaged on control cell culture substrates. DA neurons grown atop 3D GF scaffold exhibited pronounced neuronal phenotype with longer neurite extensions. The result of this study demonstrated GF as a novel scaffold for adhesion, proliferation, differentiation and maintenance of their neuronal phenotype by MSC derived DA neurons.

Chapter 2: Current approaches for symptomatic treatment of PD

Parkinson's disease (PD) is a progressive neurodegenerative disease affecting tens of millions of people worldwide and associated with socioeconomic burden [62]. The main characteristic of this disease is damage or loss of dopaminergic (DA) neuronal cells which cannot be replaced or regenerated by the nerve tissue in the patient's brain. For repairing the damaged neural function, brain electrodes can be implanted at the site of injury by open-brain surgery. Another emerging treatment is cell replacement therapy (CRT), tissue engineering patient's own stem cells which can be differentiated into neuronal cells in presence of growth factors to reduce the progression of neurodegeneration. The scaffold for transplanting the stem cells should be biocompatible, electrically conductive, and able to imitate the mechanical properties of a living tissue and should ensure not to get rejected by the host or cause any inflammation.

At present, the dopamine producing drugs like levodopa and carbidopa are the standard treatment for PD, though long-term use of levodopa is associated with the development of motor complications. Thus, the functional neurosurgery deep brain stimulation (DBS) of the subthalamic nucleus (STN) with implanted electrodes has been an effective treatment to date [62]. In this standard surgical procedure, macroelectrodes are implanted in the STN facilitating the prior functional localization of the target through intra-operative stimulation and microelectrode recordings of the activity of single neurons. Adequate targeting is confirmed through post-operative imaging following the connection and insertion of the subcutaneous stimulator under general anesthesia [62].

The symptomatic treatment with medication or DBS functional neurosurgery improve the motor symptoms and quality of life of the patient's life in the early stages of the disease, but after a few years of dopaminergic therapy, patients become progressively more disabled [63]. They suffer from the motor symptoms, such as speech impairment, abnormal posture, gait, balance problems etc. and nonmotor signs, such as autonomic dysfunction, mood and cognitive impairment, sleep problems, pain and other drug-related side effects sooner or later [63].

2.1 Biomaterial coating for brain electrodes in DBS

Ongoing research is exploring the feasibility of fabricating devices which record the electrical signals from the brain with the help of electrodes and analyzing and decoding the signals will help the paralyzed patients and amputees to move by bionic limbs [64]. The electrodes can be implanted in the patient's brain by open brain surgery or non-invasively through the blood vessel [65]. These types of devices can be used for peripheral nerve regeneration by electrically stimulating the neuronal cells and as well as in case of central nervous system by establishing connections between the transplanted 3D scaffolds. Neural implants increases our understanding about the design and application of prosthetic devices and the functional stimulation and recording from the central and peripheral nervous system [29]. These kinds of devices have shown great promise in treating neurological disorders also, such as PD.

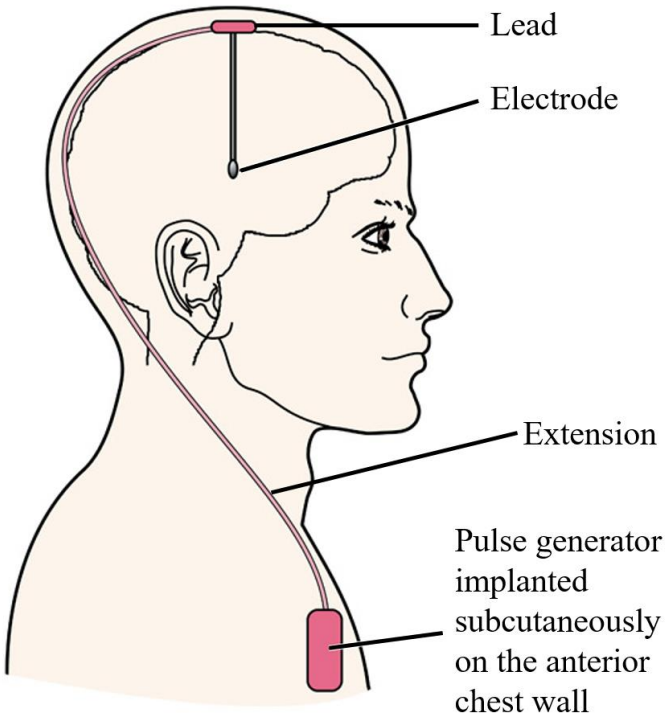

Figure 2.1: DBS electrodes are left inside the brain and the pulse generator is implanted under the skin over the chest [66]

DBS uses special electrodes to stimulate the Globus pallidus or subthalamic nucleus for the surgical treatment of PD. There are several steps to place the electrodes into the target areas of the brain during surgery. The target areas are located using computed tomography (CT) or magnetic resonance imaging (MRI) scanning [67]. Electrode recording technique is used to map and target the specific areas needed to reach at the later stage of the surgery. After identifying the correct location, the electrodes are implanted. The loose ends of the electrodes are connected to the impulse generators [67]. The electrodes for deep brain stimulation is left in the brain and are connected by a wire to a pacemaker-like device which generates the electrical stimulation being implanted under the skin over the chest as shown in Figure 2.1 [66]. In a recent research it has been proved that DBS does not relieve long-standing treatment-resistant depression any more effectively, although administering it is both safe and feasible [66].

Biomaterials incorporate extracellular matrix (ECM) molecules that have adhesive and growth promoting properties and have been used to deliver neurotrophic factors like brain derived neurotrophic factors for differentiation of stem cells into neurons. These materials have intrinsic properties that promote growth, such as the use of conductive materials to modulate the neuron's electrical and chemical activities. Biomaterials in nerve tissue engineering enhance the regenerative process by creating a growth promoting environment and directing axonal growth to reconnect nerves for functional recovery [68]. The effectiveness of the neural implants decreases with time due to glial scar tissue formation and fibrous encapsulation that electrically and mechanically isolates the device from the nerve tissue [69]. To avoid these problems, several approaches like immobilization of biomolecules on the electrode surface have been explored. Surface modification by electrostatic layer-by-layer (LbL) self-assembly technique was introduced by Decher in 1991 [70]. The underlying principle for the LbL technique is the attractive electrostatic force between a charged surface and an oppositely charged polyelectrolyte. The LbL technique is a promising approach for the construction of thin films containing macromolecules, such as proteins [71] with targeted properties onto a variety of substrates. In one study, alternating polyelectrolytes, either polyethyleneimine (PEI) or chitosan (CH), and proteins, either laminin or

gelatin, were used to fabricate multilayer films built up by LbL deposition on silicon wafers with a very thin oxide layer. Silicon wafers were chosen as the substrates because silicon is the most widely used material for neuronal electrodes. The constituents of these coatings were chosen for their general ability to promote neuronal attachment and differentiation. For instance, laminin plays a crucial role in the developing and maturing central nervous system, e.g. in cell migration, differentiation and axonal growth [72]. It has been extensively used as a substrate for the studies on the growth of neurons in vitro. These researchers used the response of chick cortical neurons to test the biocompatibility of the coatings and utilized quartz crystal microbalance (QCM) to characterize the coatings which confirmed nanoscale coatings via LbL assembly and enhanced chick cortical neuron adhesion and differentiation. There was no adverse effect after 7 days in physiological conditions and on impedance of the electrodes, confirmed by enzyme-linked immunosorbent assay (ELISA) and impedance spectroscopy. The nanoscale coating proved the potential to significantly impact the biocompatibility and performance of the electrodes [29].

In major neurological diseases such as PD, spinal cord injury and stroke, tissue engineering and regenerative medicine aims to replace the damaged tissue using different stem cells, particularly MSCs as they have shown strong potential in neuronal cell regeneration [73]. The use of stem cells in these applications has also been combined with electric stimulation [74] and biomaterial scaffolds to provide mechanical support and promote neural growth and neurogenesis at the injured areas. Electrical stimulation in treating various neurological conditions, especially Parkinson's disease is currently another significant research [67]. The development of deep brain stimulation has required designing biocompatible materials with conductive properties and the ability to support the growth of neural tissue at the implantation site. In this application, surface modification and stem cells can be used to further improve the functionality and long-term stability of the electrodes by tailoring the material-tissue interface for implantable MSC-coated brain electrode and guide the stem cells into the neuronal lineage in vivo.

2.2 Stem cell therapy

Different adult stem cells such as, neural stem cell (NSC), induced pluripotent stem cell (iPSC) and mesenchymal stem cell (MSC) have been extensively used in tissue engineering for nerve regeneration by differentiating them into neuronal cells. Among all types of stem cells, MSC seemed the most promising in respect of their capacities to differentiate toward dopaminergic neurons and to release neurotrophic factors which is very important for neurodegeneration therapy. Also, they are able to produce different molecules with immunomodulatory, neuroprotective, angiogenic, chemotactic effects and that stimulate differentiation of resident stem cells [75, 76].

In cell transplantation therapy, MSC promotes endogenous neuronal growth, decreased apoptosis, reduces levels of free radicals, encourages synaptic connections from damaged neurons and regulates inflammation, primarily through paracrine actions [75, 77]. MSCs transplanted into the brain have been demonstrated to promote functional recovery by producing trophic factors that induce survival and regeneration of host neurons [75, 77]. Therapies mainly capitalize on the innate trophic support from MSCs or on augmented growth factor support, such as delivering brain-derived neurotrophic factor or glial-derived neurotrophic factor into the brain to support injured neurons, using genetically engineered MSCs as the delivery vehicles [75, 77].

Biomaterials employed as three-dimensional (3D) scaffold provide stem cells with an appropriate microenvironment to reproduce the functions of the damaged tissue. Cell-seeded scaffolds are more effective at directing the growth by localizing the presence of growth-stimulatory molecules [78]. Hydrogel scaffolds can be categorized as natural or synthetic, such as collagen, fibrin, and hyaluronic acid are natural scaffolds being generally more biocompatible, and polylacticoglycolic acid (PLGA) or polyethylene glycol (PEG) are synthetic scaffolds having ideal mechanical and chemical properties. Main properties in designing the scaffolds for stem cell transplantation are mechanical properties, cell adhesion and biocompatibility, polymerization and degradation rate. Graphene foam (GF), a 3D porous structure, has been utilized as a promising candidate for tissue engineering scaffold as it may incorporate topographical, chemical and electrical cues to provide an environment for stem cell tissue engineering for nerve regeneration

[79]. Graphene has been used as a scaffold because it is highly biocompatible and has low toxicity having excellent electrical and mechanical properties. Table 2.1 shows how graphene and its derivatives are used in stem cell tissue engineering applications [80].

Table 2.1: Stem cell-based tissue engineering on different graphene scaffolds

Scaffold	Cell type	Result	Ref.
Reduced GO (rGO)/ TiO_2	Neural Stem Cell	The neuronal differentiation of human NSCs on rGO/TiO2 substrate is greatly higher compared to GO/TiO2 and TiO_2 substrate.	[81]
GO	Embryonic Stem Cell	GO substrate demonstrates an important enhancement of dopamine neurons differentiation	[82]
Graphene 3D foam	Neural Stem Cell	Graphene 3D foam has a greater electrical stimulation performance when compared to graphene 2D film.	[83]
Graphene coated glass	Neural Stem Cell	Graphene substrate is an excellent cell-adhesion layer during the differentiation process and induces the differentiation more	[84]
Graphene film	Neural Stem Cell	NSCs seeded on graphene film differentiate and form functional neuronal networks	[85]
Fluorinated graphene	Mesenchymal Stem Cell	Fluorinated graphene enhances cell adhesion and proliferation of human BMMSCs	[86]

The idea to create brain tissue on a dish from which we can learn about how the brain functions, is a challenging one. However, there are significant attractive benefits which completely outweigh the challenges and risks involved in this study. The value of a lab created brain tissue on a dish using a patient's own stem cells is immense, including in vitro modelling and regenerative medicine. First, tissues created from the patient's mesenchymal stem cells can be potentially transplanted back without ethical or immunological challenges. Second, such tissue on a dish models can serve as better platforms for clinical drug testing generally performed in animals, which sometimes have drastically different outcomes compared to human clinical trials. In addition, a lab created brain tissue on a dish that accurately mimics actual brain tissue would be significant for researching not only the effect of drugs, but neurodegenerative disorders like Parkinson's, Alzheimer's and ALS as well. Our long-term goal is to build 3D neural tissues on a dish that can capture in vivo neuronal functions and be useful as neural tissue on a dish for drug testing.

Chapter 3: Attenuating neurotoxicity of stainless steel used as a material for DBS, by surface modification with Graphene-oxide

Graphene-based materials, including multilayered graphene, graphene nanosheets, graphene oxide and reduced graphene oxide have been extensively utilized in electronics and energy storage/conversion systems [87]. However, an increasing interest in the field of regenerative medicine has emerged to develop nanostructured materials such as Graphene-based substrates to be used as smart interfaces for cellular studies and regenerative medicine [80, 88, 89]. This is because, nanotextured materials are believed to provide a unique physical framework, comparable to natural ECM, for cell culture [89]. So, in the field of tissue engineering, Graphene-based materials could be a promising candidate for novel scaffolds as they incorporate topographical, chemical and electrical cues in the same scaffold to provide an environment for tissue regeneration that is superior to conventional inert biomaterials [90]. Furthermore, Graphene is highly biocompatible, has low toxicity, and superior mechanical characteristics [87]. Graphene-based substrates have been recently reported to be used in bone tissue engineering [53, 89], cardiac tissue engineering [91], stem cell culture [80, 92, 93] and in neural tissue engineering as well [60, 79, 91, 93].

Inert materials such as platinum (Pt) is used for making neural electrodes which however are usually not cost effective [94]. Further these Pt electrodes require nano-textured specialized coatings for optimized performance which further increases fabrication and processing cost [94]. Therefore, there is a need for a novel low-cost coating material which will confer biocompatibility, electrochemical performance, and sustainability for application in neural interface devices. In an attempt to design a chemically and structurally stable robust electrode for chronic neural stimulation, Depan and Misra fabricated a hybrid of conducting polymer (poly(3,4-ethylenedioxythiophene) (PEDOT) and carbon nanotubes (CNTs). The PEDOT-CNT hybrid nanostructured composite coating on the SS electrodes provided biocompatibility, neuronal adhesion, neuronal outgrowth and high charge injection capacity [95]. Others reported, poly(ethylene glycol)-poly(ε-caprolactone) (PEGPCL) hydrogel–poly(ε-caprolactone)

neurotrophin-eluting hydrogel–electrospun fiber composite coatings for multi-electrode arrays which enhanced long-term device performance and function [96]. However, inclusion of a growth factor and polymer has its own challenges in terms of cost and manufacturing burden, and limited life-span of the growth factor incorporated. So a single component coating based on a polymer-free approach would be ideal for such applications to avoid toxicity associated with polymers [97]. Thus, in this study we aimed to develop graphene oxide (GO) as a novel polymer-free, biocompatible and strongly adherent coating on 316L SS implant surfaces for neuronal cell culture applications.

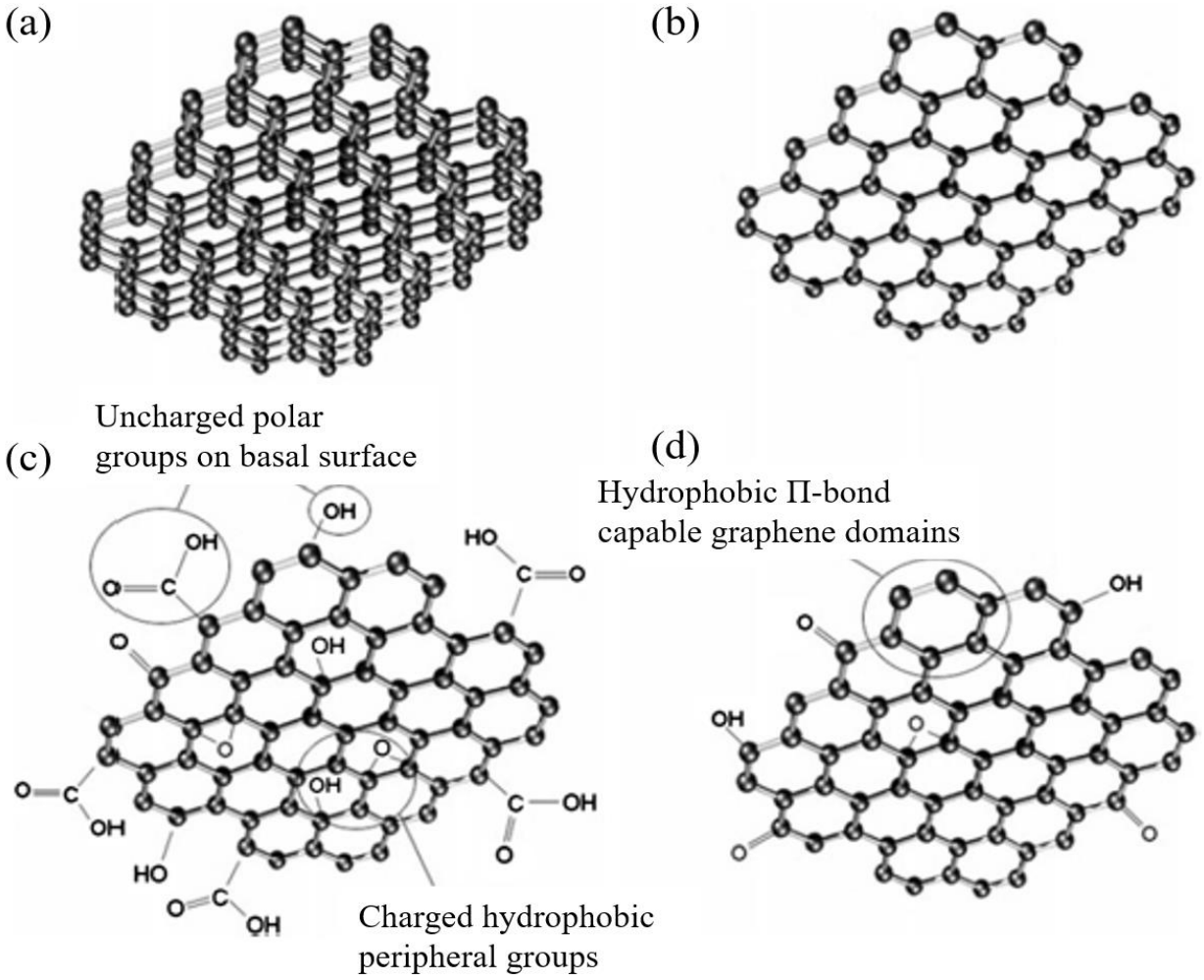

Figure 3.1: Some members of graphene family, shown in (a) Few-layered graphene, (b) graphene nanosheet, (c) graphene oxide, and (d) reduced graphene oxide (rGO) [98]

Graphene Oxide (GO) sheets are monolayers of carbon atoms that have oxygen atoms, -OH groups and –COOH groups attached forming dense and unique honeycomb structures [99] with applications in biomedical field [49-51, 56, 100-105]. These functional groups enable GO to be readily dispersed in water [106]. Some members of graphene family is shown in Figure 3.1, such as few-layered graphene, graphene nanosheet, graphene oxide, and reduced graphene oxide (rGO) [80]. The aim of this study was to culture SHSY-5Y cells [59] to show cell adhesion, proliferation and decreased expression of ROS signaling indicative of the mitochondrial stress in neurons affected by PD, atop Graphene-oxide coated SS meshes (Figure 3.2).

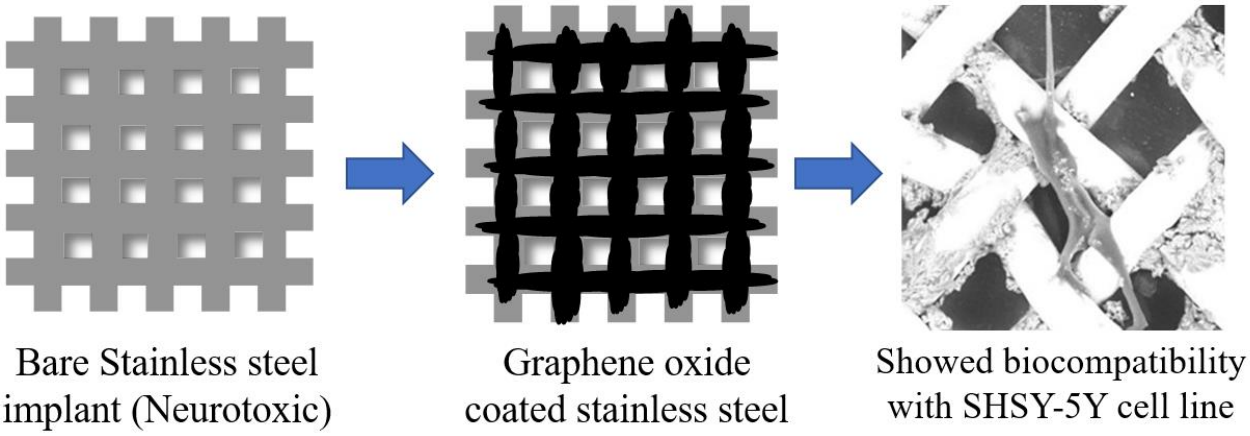

Figure 3.2: SHSY-5Y neuroblastoma cells grown on graphene oxide coated stainless steel mesh

GO was immobilized onto 316L SS surfaces using a carbodiimide reaction by surface treatment with (3-amminopropyl)triethoxysilane (APTES) [48]. GO coated 316L SS surfaces were prepared, characterized and used to culture SHSY-5Y neuroblastoma cells [107] to assess the overall biocompatibility of the modified substrate. Further this method of GO-coating can be adapted to other metallic implants where the development of such protective and biocompatible coatings is essential [55, 108]. Results from this study showed that GO-coated SS neural electrodes (Figure 3.2).

3.1 Materials and methods

Graphite flakes (~150 μm), APTES (99%), 1-(3-Dimethylaminopropyl)-1'-ethylcarbodiimide hydrochloride (EDC), N-Hydroxysuccinimide (98%) (NHS), Atto 495 NHS ester, was obtained from Sigma-Aldrich (St. Louis, MO, USA). 0.25% Trypsin/EDTA and Phosphate Buffered Saline (PBS, 1X) was obtained from Sigma. 316L SS wire cloth mesh (200 x 200 Super-Corrosion Resistant type 316L SS Wire Cloth, 0.0016" Wire Diameter, 46% open area, McMaster-Carr, Los Angeles, CA, USA) was used to mimic surgical grade 316L SS implant surfaces. Solid strips of the same material (316L SS, thickness 0.015", width 1" and length 24"; McMaster-Carr) were used for contact angle, nanoindentation and film thickness measurements.

3.1.1 Preparation and characterization of GO

GO was prepared by a modified Hummer's method as done previously [106, 109, 110]. Briefly, a 9:1 mixture of sulphuric acid/ phosphoric acid (H_2SO_4/H_3PO_4) was added to a mixture of graphite flakes and potassium permanganate ($KMnO_4$). The reaction was then heated to 50^0C with stirring for 12 hr, and consecutively cooled and poured onto ice with 30% hydrogen peroxide (H_2O_2). The mixture was sifted and filtered; it was later centrifuged and the supernatant was decanted away. The remaining solid GO was washed consecutively with Milli-Q water, 30% H_2O_2, and ethanol (C_2H_6O); for each wash, the mixture was again sifted and filtered. After multiple washes, the remaining material was coagulated with ether $(C_2H_5)_2O$ and the resulting suspension was filtered. The final solid product was freeze-dried under vacuum overnight. All chemicals used in the in-house synthesis of GO was procured from Thermo Fisher Scientific, Hampton, NH, USA.

FTIR analysis: Fourier transform infrared spectroscopy (FTIR) was used to reveal information about the molecular structure of GO prepared in-house in comparison with published literature. Attenuated total reflectance (ATR)-FTIR spectra of a representative GO sample was acquired using a Perkin-Elmer, Spectrum 100, Universal ATR Sampling Accessory within the range of 650-3650 cm^{-1} in transmittance mode [111]. Spectral manipulations were performed using the spectral analysis software GRAMS/32 (Galactic Industries Corp., Salem, NH, USA). External

reflection FTIR was recorded on a Specac grazing angle accessory using an s-polarized beam at an angle of incidence of 40^0 and a mercury cadmium telluride (MCT/A) detector. A piranha-treated silicon wafer was used as the background.

3.1.2 Stainless Steel mesh treatment prior to GO immobilization

Surface modification was performed on the 316L SS meshes as follows. The mesh was cut into 2 cm × 1 cm pieces and sonicated in acetone for 20 min followed by air drying and consecutive heating (250^0C, 1 hr). The pristine cleaned 316L SS meshes were denoted as NHT (no heat treatment), and the heated ones as HT (heat treated) respectively.

316L SS silanization with APTES: For modifying the 316L SS surfaces to promote GO immobilization, it was necessary to covalently introduce a layer of functional silane groups onto the surfaces. To enable this reaction, all samples were submerged in a 10% v/v solution of APTES/Xylene (Sigma) with continuous stirring for 24 hr to facilitate the carboxyl (-COOH) groups of the GO to covalently bond to the amine ($-NH_2$) groups.

3.1.3 GO immobilization and retention

Atto 495 NHS-ester dye solution was made by adding 5 µl of the dye solution in DMSO (2 mg/ml) to 95 µl of bicarbonate buffer (0.1 M, pH 8.3). 100 µl of this prepared solution was laid onto each mesh treated with APTES to confirm the attachment of amine groups and incubated at room temp for upto 2 hr after which they were imaged using a fluorescence microscope (Nikon Eclipse Ti, Nikon Instruments Inc., Melville, NY, USA). Fluorescence and bright field images were acquired and later merged with identical parameters using ImageJ.

Upon confirmation of the amine groups on the 316L SS meshes, a saturated solution of 2 mg/ml of GO/Milli-Q water was made to coat all samples by eliciting a carbodiimide reaction using the crosslinking agents EDC and NHS [112]. Samples were submerged in 10 ml of the GO/Milli-Q water solution, 0.8 grams of EDC and 1.2 mg of NHS were added at room temperature (25^0C) with vigorous stirring for 24 hr. The GO-coated meshes were then heated in the oven

(250^0C, 1 hr) to stabilize and bind the GO coating with underlying substrate. All chemicals used in this step were procured from Sigma.

3.1.4 Characterization of the GO-coating

XRD for confirmation of GO-coating deposition

To investigate the efficacy of the coating and the phase assemblage of the GO and the APTES coated 316L SS strips, samples were examined by X-ray diffraction (XRD). For the XRD, the samples were scanned using an X-ray of Cu source (CuKα, wavelength: 1.54056 Å) for a 2 theta range from 5° to 90° at a scanning rate of 2°/min with an increment (step size) of 0.05°. The XRD machine (D8 Discover, Bruker's diffractometer, Germany) was operated in locked-coupled mode at 40 kV voltage and 40 mA currents.

SEM analysis for probing morphology of GO coated surfaces

To image the morphology of the deposited GO-film, scanning electron microscopy (SEM) was used. Samples were visualized using SEM (S-4800, Hitachi, Japan) at voltages of 5KV.

Measurement of contact angle

For measuring contact angles, GO was deposited onto 316L SS strips using similar immobilization procedures as used for the meshes. Water contact angles of the GO-coated surfaces were measured at room temperature and humidity using a standard goniometer (Model 250-F4, Ramé-hart, Succasunna, NJ, USA) based on the sessile drop method. For each value reported, the mean and standard deviation of at least 10 measurements from the same sample surface were recorded. For each case, 2 representative samples were prepared and analysed.

Estimation of coating thickness

For measuring GO-coating thickness, GO was immobilized onto 316L SS strips using similar procedures as used for the 316L SS meshes. Cross section of the GO-coated samples was visualized using SEM (Hitachi TM-1000 Tabletop Microscope, Tokyo, Japan) at 1000× to 5000×

magnification. Acquired images were analyzed using ImageJ (NIH) to calculate average thickness of the deposited GO-coatings.

Nanoindentation for mechanical analysis

A dynamic nanoindentor (TI-750H, Hysitron Inc. MN, USA) with a diamond tip of diameter of 200 nm was used for the indentation of the GO coating. Furthermore, hardness and elastic modulus were calculated using area under the loading and unloading curve i.e. plastic and elastic work of the indentation, respectively. The value of total work of indentation (a sum of plastic and elastic work) was substituted in the following equation to calculate the hardness of the GO coating [113].

$$H = \frac{kP_m^3}{9W_t^2} \text{.....(1)}$$

where, k is a constant equal to 0.0408 (for a three-sided Berkovich pyramidal indenter). P_m and W_t, are the maximum load and total work of indentation.

The standard method to measure the elastic modulus of the coating is by the analysis of the unloading curve. This is due to the fact that even for a plastic deformation during loading, the initial part of the unloading curve exhibits the elastic nature of the material. Therefore, slope of initial part of unloading curve can be used to calculate the elastic modulus of the material using following equation [114, 115].

$$\frac{1}{E_r} = \left(\frac{1-\nu^2}{E}\right) + \left(\frac{1-\nu_i^2}{E_i}\right) \text{.....(2)}$$

where, E_r, E, and E_i are the reduced elastic modulus, elastic modulus of the substrate i.e. graphene oxide coating, and elastic modulus of a diamond indenter (= 1141 GPa) [114]. ν and ν_i, are the Poisson ratio of the graphene oxide (= 0.165 [116]) and the indenter (0.07 [114]).

The reduced elastic modulus can be calculated using following relation [114, 117],

$$E_r = \frac{\sqrt{\pi}}{2}\frac{S_{max}}{\sqrt{A}} \text{.....(3)}$$

where, S_{max} and A are the slope of the unloading at the starting point i.e. at the point of maximum loading and the projected area of indentation. The projected area of indentation is defined in terms of contact depth, h_c and can be expressed as [114],

$$h_c = h_{max} - \varepsilon\frac{P_{max}}{S_{max}} \text{.....(4)}$$

where, ε is a constant that depends on the geometry of the indenter and for a sharp Berkovich indenter this value is 0.75 [117]. Therefore, for the present case of nano-indentation, equation 4 was rewritten as,

$$h_c = h_{max} - 0.75\frac{P_{max}}{S_{max}} \text{.....(5)}$$

It is already known from the load-displacement curve that $h_c < h_{max}$ [117]. The contact area of the indentation is a function of the contact depth (h_c) i.e. $A = A(h_c)$ [114] and for a perfectly sharp Berkovich indenter, $A(h_c) = 24.5\, h_c^2$.

Therefore, A in equation 3 was replaced with h_c to calculate the elastic modulus of the coating "E" using equation 2. Modified equation 3 shown in 6 was used to estimate Elastic Modulus of the deposited GO coatings onto SS substrates.

$$E_r = \frac{\sqrt{\pi}}{2}\frac{S_{max}}{4.95h_c} \text{.....(6)}$$

3.1.5 Cell culture on GO coated surfaces

Adhesion and proliferation of SHSY-5Y neuroblastoma cells atop GO-coated surfaces

In preparation for cell culture, the precut meshes including bare, APTES-treated and GO-coated were washed first in 70% ethanol, followed by PBS (1X) and air dried under a sterile laminar flow hood. After drying, samples were transferred to wells (one mesh/ well) in a 24 well plate (Corning, NY, USA). SHSY-5Y cells, a generous gift from Dr. Mahesh Narayan from Chemistry department at UTEP were seeded atop these meshes following procedures described. SHSY-5Y is used as a model of in vitro neurodegenerative disease studies because it has biochemical properties of human neurons in vivo [107]. Further, since these cells are tumour derived, they have the ability to continuously grow and divide [107]. The cells can be differentiated to provide mature neuron-like phenotype [107].

SHSY-5Y cells were grown in DMEM-F12 (1:1; Gibco, Thermo Fisher Scientific), supplemented with 10% heat inactivated FBS (Gibco), 2 mM L-glutamine, 100U/ml penicillin and 100 mg/ml streptomycin all from Gibco. Prior to the mesh experiment, the cells were cultured and stabilized for several passages at 37°C, 5% CO_2. Confluent T-25 flasks of SHSY-5Y cells were trypsinized and extracted for further experiments.

Pre-cleaned bare, APTES treated and GO-coated 316L SS meshes were further cut into 8 mm × 8 mm (n=3 for each case) and were placed into the media per well of a 24 well plate. Then the cells were added to these respective wells at a density of 10,000 cells/well with 2 mL of media per well. The seeded cells on meshes in wells were then incubated (37°C, 5% CO_2) for a period of up to 72 hr.

After 72 hr, cells at the bottom of the wells were stained using DAPI (Vector labs, Burlingame, CA, USA) and Ethidium homodimer-1 (Dead cell stain, Invitrogen, Thermo Fisher Scientific) and imaged using an inverted fluorescence microscope (ZEISS Axio Observer, ZEISS, NY, USA).

On the other hand, cell proliferation on the meshes was estimated as described. Meshes seeded with cells were carefully transferred to unused wells, gently rinsed with PBS, overlaid with

1 mL of 0.25% trypsin-EDTA per well and incubated at 37°C for 10 min. Extracted cells were pelleted by centrifugation, and counted using a hemocytometer throughout the entire culture period after 72 hr of culture following published procedures [118]. Similarly, cells that adhered to the plastic wells for the respective mesh samples were also trypsin-extracted and estimated after 72 hr of culture. Mean values obtained by averaging values from at least 3 samples per case were reported for cells adhered onto plastic wells and mesh surfaces respectively for each case reported, in comparison to controls (plastic only). All cell culture experiments were repeated twice (n = 3 for each experiment).

En-face images of the meshes seeded with cells were acquired using SEM following published procedures to confirm cell adhesion onto the meshes [119]. For sample preparation, cells on meshes were histologically fixed using 4% paraformaldehyde (Sigma, 4°C, overnite), and then dried under a constant laminar air-flow in a fume hood. Dried samples were coated with gold (2–3 min) in a sputter coater (Quorum EMS150R ES, Quorum Technologies Ltd., UK) and visualized using SEM (Hitachi TM-1000 Tabletop Microscope) at 1000× to 5000× magnification.

ROS detection and quantification

In order to establish GO's role in modulating inflammatory responses if any, reactive oxygen species (ROS) expression in SHSY-5Y cells cultured atop GO-coated meshes were analyzed using immunofluorescence following published procedures [120]. Levels of ROS in SHSY-5Y cultured in vicinity of GO-coated surfaces were assessed using conversion of non-fluorescent dihydroethidium (DHE: Sigma) to fluorescent ethidium bromide. Cells cultured in wells along with bare uncoated 316L SS (controls) and GO-coated meshes were incubated with DHE (10 μM) for 15 min at 37°C under dark conditions and imaged within 5-7 min. Cells cultured in wells that did not contain any meshes served as negative controls. After 15 min of incubation, cells were visualized using an inverted fluorescence microscope (ZEISS Axio Observer).

***Statistical analysis*:** All samples were present in triplicate unless otherwise mentioned. Data are expressed as the mean ± standard deviation. Student's t-test was performed to determine

if the averages of any two sample datasets compared were significantly different. p-values less than 0.05 were considered significant wherever reported.

3.2 Results and Discussion

3.2.1 Silanization of bare 316L SS surfaces

To modify the inorganic surface of the 316L SS mesh to promote GO immobilization, the initial reaction that occurred on the 316L SS mesh was for the –Si-O-Si of the silane coupling agent (APTES) to bond to –OH groups in GO on the mesh's surface (Figure 3.3 (I)) [112, 121]. APTES is used on an routine basis for surface coatings where silanization is needed [122].

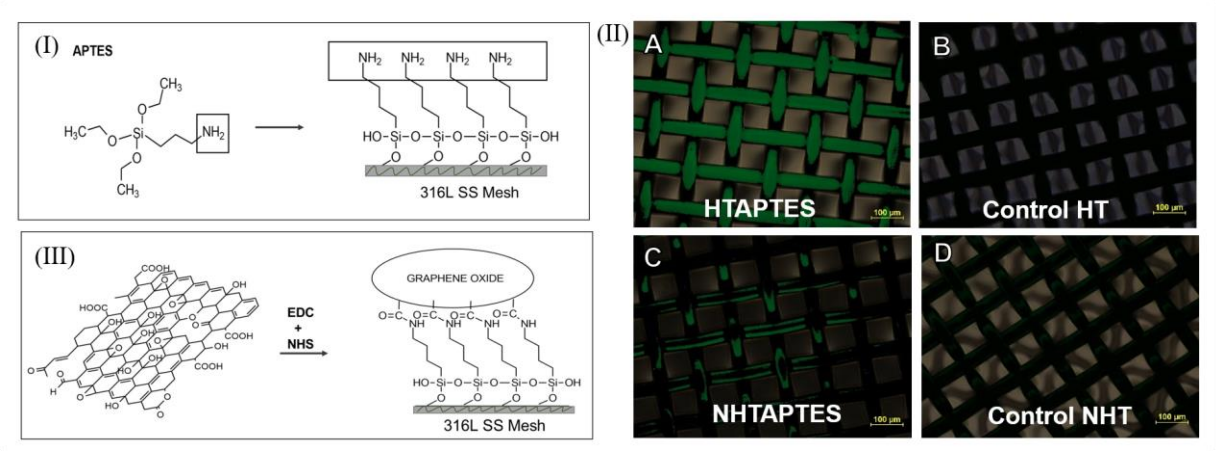

Figure 3.3: (I) Schematic for deposition of NH_2 groups on 316L SS meshes. (II) Confirmation of NH_2 groups on the 316L SS meshes. Shown in panel (A-D) are Atto 495 dyed 316L SS meshes, scale bar = 100 µm. In (A) the meshes were heat and APTES treated (denoted as HTAPTES); (C) the pristine cleaned 316L SS meshes were not heat treated but treated with APTES (denoted as NHTAPTES). Controls for all these treatments are shown in (B) and (D). (III) The chemical crosslinking scheme for GO adhesion.

3.2.2 Confirmation of NH_2 group immobilization

Atto 495 NHS-ester die treatment confirmed the presence of amine groups on treated surfaces. The mesh samples which were heat treated reacted the most with APTES compared to

non-heat-treated controls. The heat-treated samples retained the maximum amount of NH_2 groups confirmed visually compared to controls (Figure 3.3 (II)). Therefore, heat treatment was used as an optimized prior treatment for 316L SS meshes that were then reacted with APTES to bind NH_2 groups.

3.2.3 Confirmation of GO immobilization

FTIR spectra analysis revealed the structure and functional groups of the in-house synthesized GO [123, 124] (Figure 3.4 A). The spectrum showed the presence of C=O stretching vibration centred at 1728 cm^{-1}, graphene sheet aromatic C=C stretching vibration at 1622 cm^{-1}, broad O–H stretching at 3400 cm^{-1}, C-OH bending at 1368 cm^{-1}, C-O stretching at 1045 cm^{-1}, C–OH stretching at 1222 cm^{-1}. The presentation of oxygen-containing functional groups, such as –COOH, –OH, epoxide, and alcoxide confirmed that the synthesized compound was GO in consistence with other published evidences [106, 109, 121]. Also, the –COOH, –OH was reacted completely with the $–NH_2$ groups present on the 316L SS surface from the APTES treatment, leading to GO-immobilization. Therefore, these GO-coatings are not expected to be thrombogenic when developed for in vivo use [55].

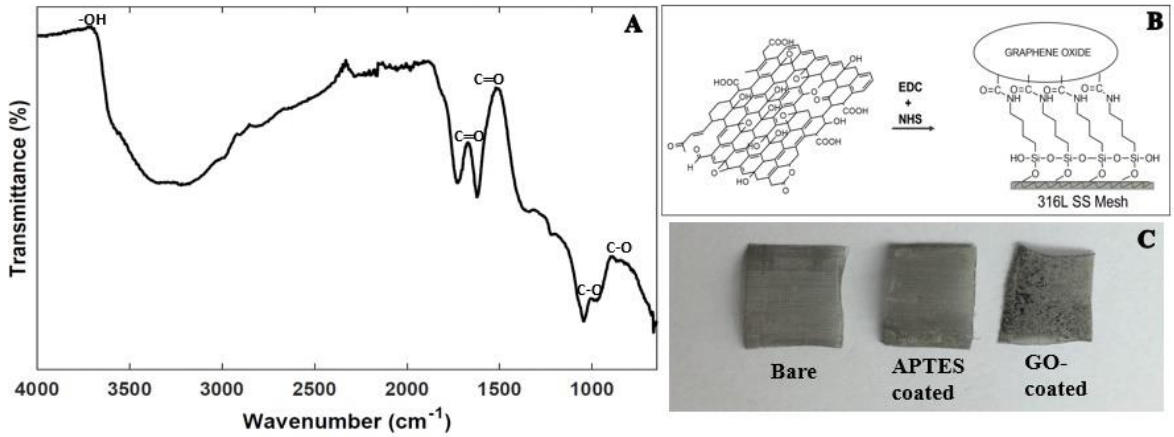

Figure 3.4: Shown in (A) is a representative FTIR spectrum of GO prepared in-house. The chemical crosslinking scheme for GO adhesion is depicted in (B). GO coating was visually confirmed as shown in (C) in comparison with uncoated and APTES treated 316L SS meshes. Shown in (B) is the schematic for GO-immobilization onto 316 L SS meshes and in (C) are pristine 316 SS meshes (left), APTES-coated meshes (middle) and GO-coated meshes (right).

A saturated aqueous solution of 2 mg/ml GO was used to coat all 316L SS samples as depicted in Figure 3.4 B. GO deposition was visually confirmed on the 316L SS meshes compared to non-coated meshes (Figure 3.4 C). GO-coated meshes were then washed, to remove unreacted GO and then used for further experiments.

3.2.4 Confirmation of the GO-coating

Three samples in each category including bare (uncoated) 316L SS, GO-coated 316 L SS, and APTES coated 316L SS were analysed using XRD from which one representative spectrum from each case was depicted (Figure 3.5). The XRD spectra of bare 316L SS revealed the presence of diffraction peaks matching with the austenite phase with three major diffraction peaks corresponding to 111, 200, and 220. No other phase was identified in the detection limit of the XRD (Figure 3.5). The XRD spectra of GO coated samples confirmed the presence of signatory diffraction peaks of GO with very low-intensity diffraction peaks corresponding to substrate material (316L SS). In addition to this, peaks corresponding to reduced GO were also found. The XRD of APTES coated samples confirmed the presence of diffraction peaks corresponding to SiO_2 (ICDD pdf # 890735). In this case, the highest intensity diffraction peaks were of the stainless-steel substrate. However, no other phase than SiO_2 and stainless steel were noted.

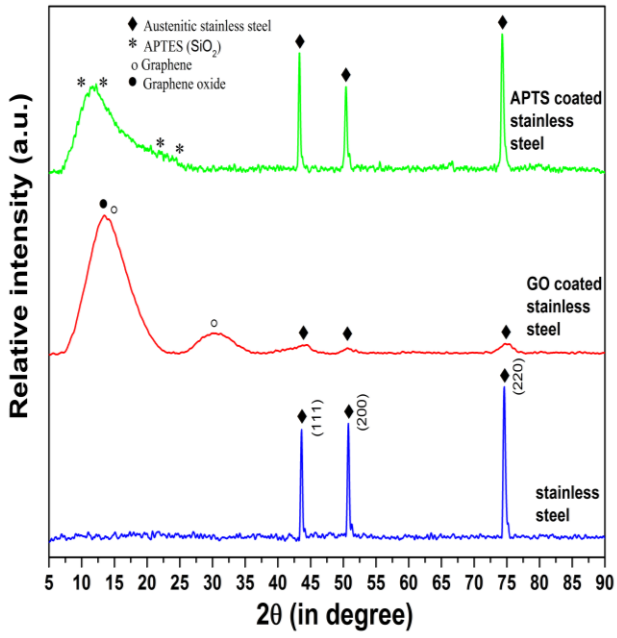

Figure 3.5: XRD of bare stainless steel, GO coated stainless steel, APTES coated stainless steel substrates, showing the presence of GO and APTES on the substrate surface.

In both cases, for GO- and APTES-coated 316L SS (ICDD pdf # 033-0397) samples, the absence of any other diffraction peaks except the diffraction peaks of the base material and coating confirmed the purity and efficacy of the coating and coating-method, respectively.

In addition to GO, the presence of reduced GO can be related to the in-house synthesis of GO which involved the oxidation of graphite [123, 124]. In the case of GO coating, the peak corresponding to GO was of highest intensity among the other phases. This confirmed GO as the most abundant phase in the stable coating of GO on the 316L SS substrates. However, in the case of APTES coated samples, the coating was not very uniform, which was confirmed by the presence of high intensity diffraction peaks of austenite phase of substrate 316L SS. To fix this issue, pristine cleaned 316L SS samples will be polished, surface smoothness confirmed using SEM and then APTES treated in future to promote deposition of a uniform coating of APTES.

3.2.5 Morphology of the GO coating

SEM revealed that though the GO-coating was retained all over the 316L SS mesh surface, it seemed non-homogenous (Figure 3.6). The junctions of the meshes seemingly showed greater amounts of GO deposited compared to struts (Figure 3.6). We attempted to graft GO onto mesh surfaces simply stir-coating and did not employ any special means to make the coating uniform. In succeeding studies, we will employ means to make the GO-coating uniform on the 316L SS surfaces using electrophoretic deposition or spin coating. Further polishing the 316L SS surfaces prior to coating will promote uniform APTES coating which will in turn facilitate uniform homogenous GO coating.

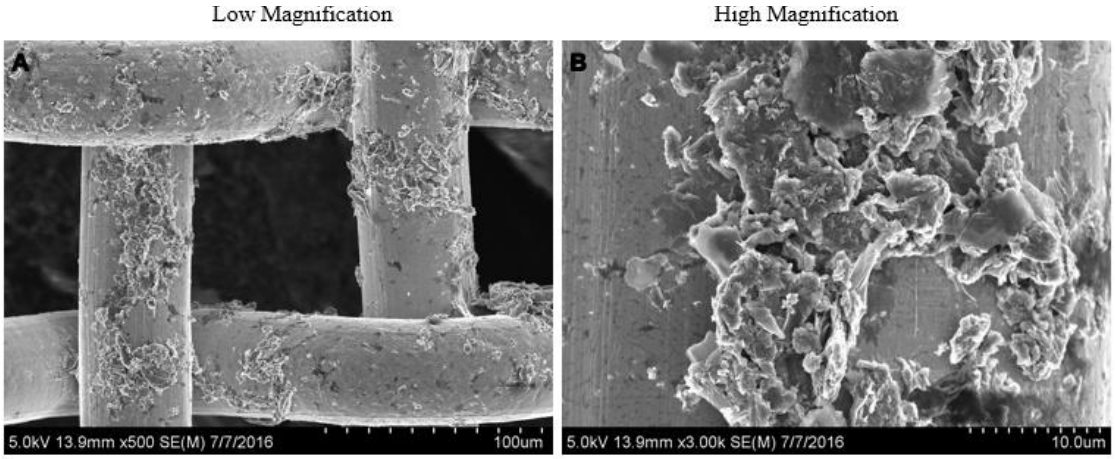

Figure 3.6: Representative SEM images of GO-coated meshes at various magnifications.

Nevertheless, the GO-coating appeared to possess surface-roughness on a nanoscale (Figure 3.6). No such nano-scale roughness was noted in meshes coated with APTES or in non-coated control 316L SS substrates.

3.2.6 Surface hydrophilicity is retained after GO-coating

The surface hydrophilicity retained by the GO-coating was revealed from contact angle investigations (Figure 3.7 A). The absorbed GO-coating decreased the contact angle to

22.31°±3.76 in comparison to bare untreated samples (33.12°±0.75) (p=0.009). Silanized APTES-coated substrate showed an average contact angle of 61.33°±0.19. Therefore, the GO-coating conferred hydrophilicity to the coated 316L SS substrates probably due to the nano-topographic roughness (Figure 3.7 A).

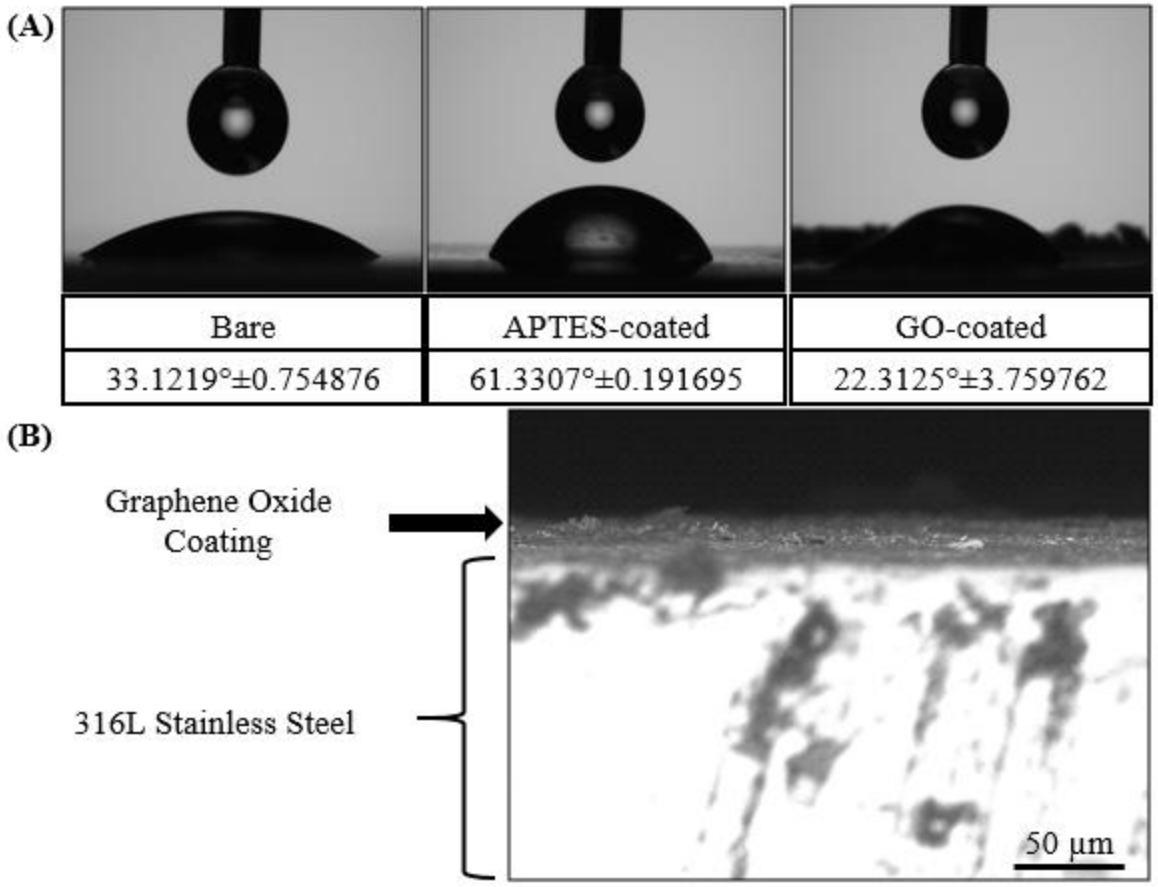

Figure 3.7: Shown in (A) are the representative images and the results of contact angle investigations. GO-coated surfaces maintained hydrophilicity are shown above. (B) Representative SEM image of GO-coating on 316L SS strip.

3.2.7 GO coating thickness

For the samples analysed using SEM (Figure 3.7 B), the average thickness of the GO-coating was 11.24 ± 1.23 µm. Earlier studies have shown that a single layer of GO sheet is 0.52

nm in thickness [125]. So, it was concluded that a multi-layered coating of GO was deposited due to APTES treatment and GO immobilization on the 316L-SS meshes. Others investigating multi-layered GO films have found these coatings to be impermeable to all gases, liquids and aggressive chemicals thereby protecting the underlying surface from interfacing with corrosive environments [54].

3.2.8 Hardness and Modulus of elasticity of the GO-coating

Inside complex in vivo environments, applied biomaterial coatings usually play a role in the targeted performance of a biomaterial, such as bioactivity [126]. Therefore, apart from the biological properties, the reliability of such biomaterial coatings can be affected by its mechanical properties, such as hardness and elastic modulus. A technique such as nanoindentation can be used to measure the mechanical properties of applied coatings including hardness and elastic modulus by deforming it on a very small scale. For all GO-coated samples analyzed, the average value of hardness was 19.950 ± 0.248 GPa and the average value of elastic modulus was 570.560 ± 25.659 GPa.

The measured value of hardness and elastic modulus of GO coating was higher than the hardness and elastic modulus of other common implant coatings on 316L SS [123, 124, 127]. Substrate hardness plays an important role in the determining the wear and tear properties of a material and generally, a higher hardness means a lower wear rate [128]. Therefore, on the basis of nanoindentation results it is expected that the GO-coating will exhibit significantly lower coefficient of friction and lower wear rate as well, when implanted in vivo. Besides, studies have also shown that substrate stiffness, a property related to hardness and elastic modulus is an important growth cue for neuronal outgrowth and differentiation [129]. Stiffer substrates with enhanced elastic modulus increased cultured neuronal network activity atop these substrates as

shown by other studies [129]. Therefore the GO-coating should be beneficial for neuronal outgrowth, and may even be beneficial in studies to probe the behavior of diseased or damaged Parkinson's neurons [96].

3.2.9 Biocompatibility of the GO-coating

To determine the overall biocompatibility of the GO-coatings, SHSY-5Y cells were cultured atop these substrates. From other published studies using these cell types, it is already known that GO is non-cytotoxic and promotes cell adhesion and differentiation in SHSY-5Y cells [51]. In line with these published reports, it was seen that SHSY-5Y cells adhered well onto GO-coated surfaces (Figure 3.8 A, B, C), to a greater extent than on bare or APTES coated 316L SS surfaces (Figure 3.8 D). Cells on the GO-coated surfaces appeared to express a mature neuronal morphology and phenotype (Figure 3.8 A). Cells attached and grew on both the plastic wells and the meshes (Figure 3.8 D), however total number of proliferating cells at the end of culture was much lesser in wells that contained bare and APTES-coated meshes in comparison to GO-coated meshes or plastic well controls (Figure 3.8 D). When compared within wells with meshes, cells adhered and grew significantly more on GO-coated meshes in comparison with bare ($p=0.001$) and APTES-coated ($p=0.006$) meshes (Figure 3.8 D). These results implied that GO-coatings enhanced SHSY-5Y cell adhesion and proliferation thereby improving the functionality and behaviour of these cells when seeded on GO. On the other hand, cells that were cultured in the vicinity of the meshes including bare, APTES- and GO-coated showed maximum number of dead cells in wells that contained the bare non-coated meshes, in comparison to the other cases (Figure 3.9). This result further supported the fact that GO was not cytotoxic.

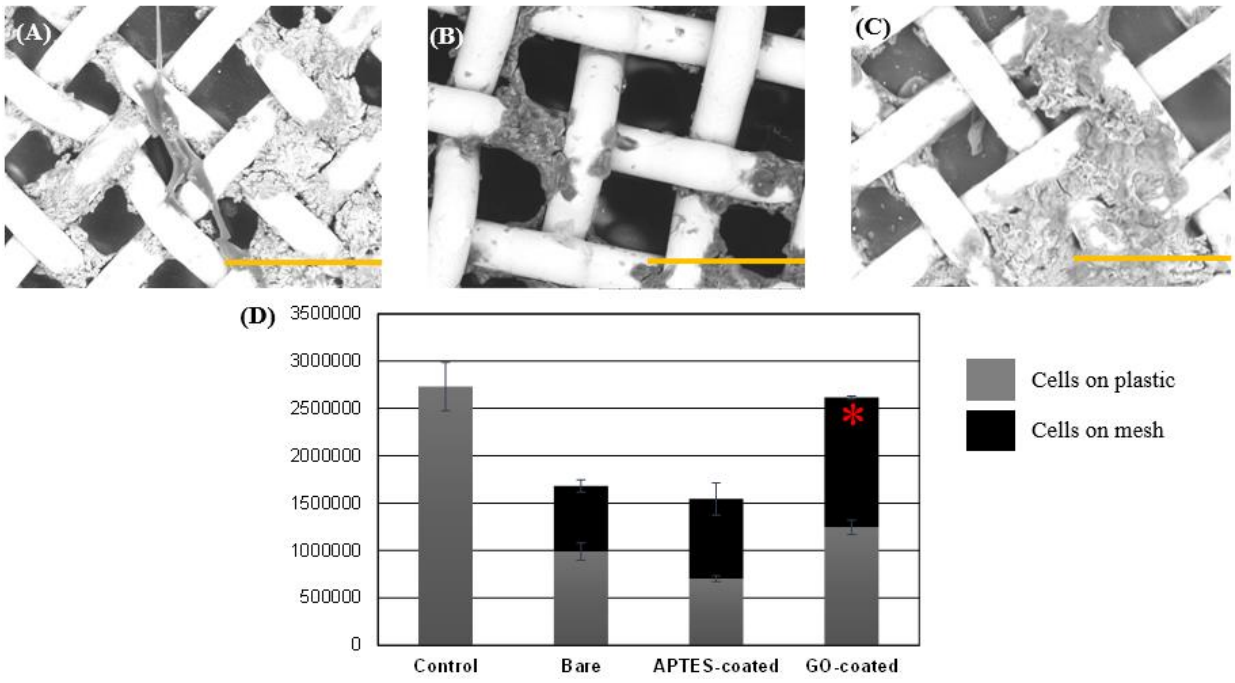

Figure 3.8: Representative SEM images of SH5YSY cells grown atop GO-coated meshes in (A) (B) and (C). Depicted scale bars are a 100 µm. (D) Confirmation of cell proliferation on GO-coated meshes. Significantly greater no. of viable proliferating cells were detected on GO-coated meshes after 72 hours of culture compared with bare and APTES-coated meshes.

SHSY-5Y cells cultured in the vicinity of GO-coated meshes exhibited lesser number of cells that showed less intense red DHE fluorescence compared to cells cultured on pristine 316L SS meshes. Therefore, culturing cells on GO-coated 316L SS meshes did not activate signalling pathways that lead to ROS activation and cellular damage. In a study by Min Lv et al. [51], SHSY-5Y cells cultured atop GO nanosheets showed no cytotoxicity associated with the GO, which further enhanced the differentiation of SHSY-5Y induced-retinoic acid (RA) by increasing neurite extension length and the expression of neuronal marker MAP2. Results from this study and others [49] strongly imply a role of GO-coatings as applications for neurodegenerative diseases. Further,

we have shown that neuronal cell culture atop GO actually mediates ROS expression which could lead to its application as coating material for neural implant electrodes.

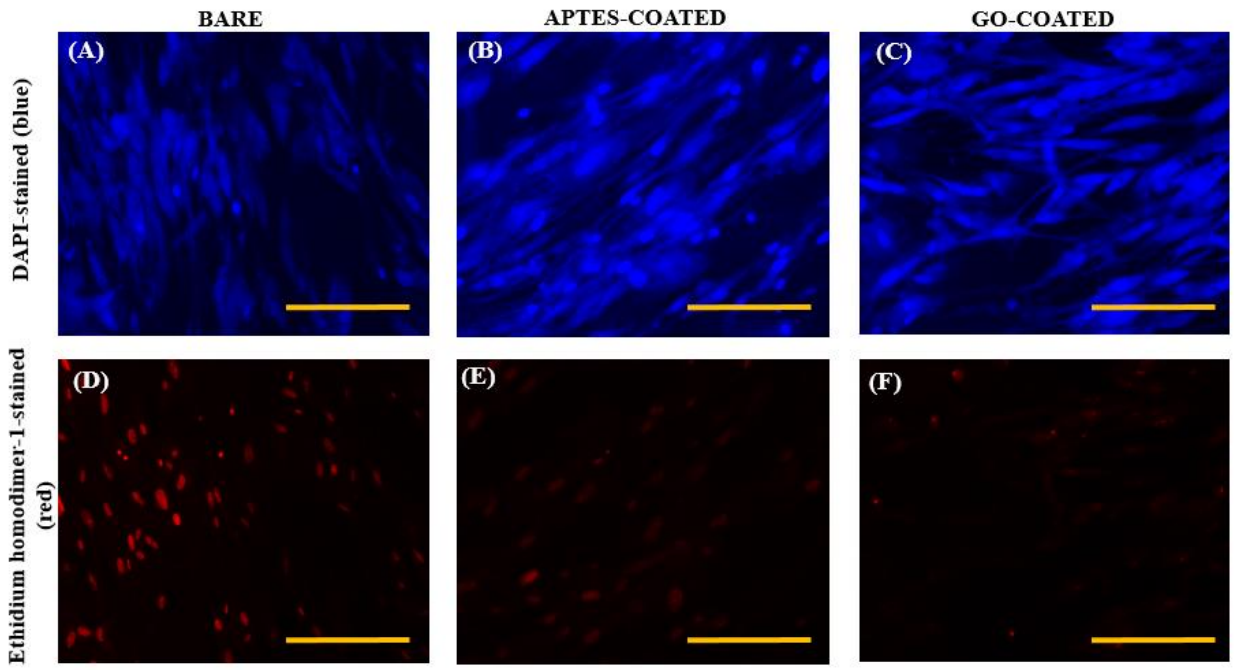

Figure 3.9: Cells cultured in the vicinity of bare-316L SS (A, D), APTES-coated (B, E) and GO-coated samples (C, F) stained using DAPI (top panel) and a dead cell stain, Ethidium homodimer-1 (bottom panel) depicted in representative images. Maximum no. of cells appeared dead when cultured in the vicinity of bare-316L SS samples but not the other cases. Scale bar is 100 μm.

3.3 Conclusion

In conclusion, GO coated surfaces did not exhibit any significant in vitro toxicity for SHSY-5Y cells and reduced their ROS expression, confirming its biocompatibility. Further, GO coatings were found to be stable, non-reactive and added surface roughness to the implant surfaces which permitted cell adhesion, spreading and proliferation, without inclusion of any additional neuronal growth factors [96]. All of these characteristics make GO suitable for 316L SS biomedical implants and devices. This study significantly advanced the existing knowledge on the biological properties of GO-coating and its possible applications in biomedical field.

The procedure employed for making GO-coatings in this study is fairly facile, inexpensive and less time consuming. In addition, our technique for making GO-coatings is aqueous based, easily scalable, cost effective and allows room temperature fabrication. The finding of these results can be extended to other studies wherein such hydrophilic and corrosion defiant GO-coatings also have immense potential as a protective shield for oxidation prone active metal surfaces.

Chapter 4: Stem cell differentiation for targeted DA neuron transplantation

Stem cell based tissue engineering has tremendous potential of long-term restoration of all types of tissues including skin, cardiac, bone and nerve by gene therapy [130]. Though biocompatible metals and soft natural and synthetic polymers have been extensively used for fabricating brain electrode and cell transplant scaffold in tissue engineering and regenerative medicine research, graphene has shown to accelerate stem cell differentiation being mechanically robust, biocompatible, flexible and electrically conductive. Graphene was used as a neuro-interface electrode without altering or damaging signal strength or formation of scar tissue [131].

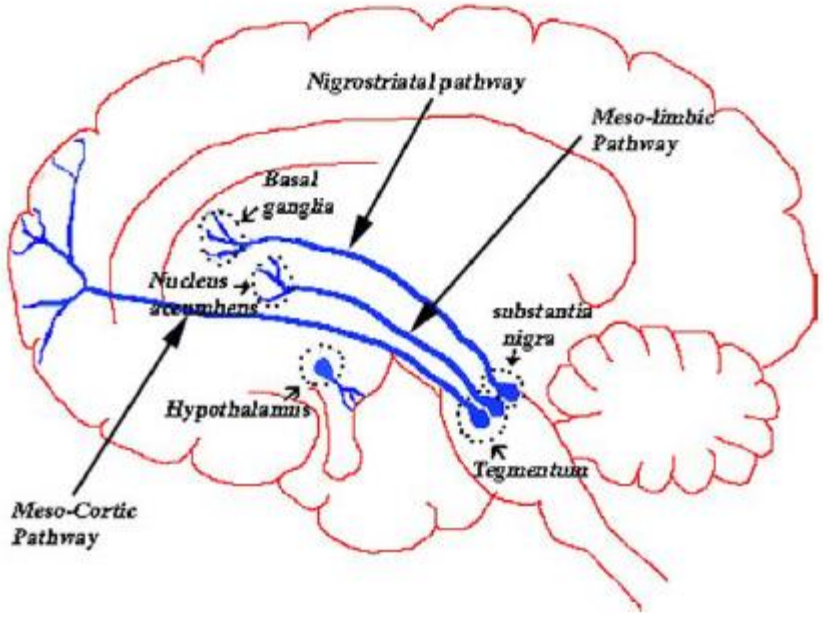

Figure 4.1: DA neuron pathway in the mid-brain [132]

Cell transplantation therapy involves culturing the undifferentiated stem cells in vitro and then implant the cells at the brain injury site with protein, growth factors and neurotrophic factors for direct differentiation into neuronal cells. The stem cells can be differentiated in the lab to model different neurodegenerative disorders in a dish to investigate the disease nature and possible

treatments before performing animal study and clinical application [133]. Figure 4.1 shows the representative image of the DA neuron pathway in the human mid-brain [132]. In case of neurodegenerative disease like Parkinson's, large portion of dopamine producing cells are lost in the mid-brain. So, artificially created neural tissue needs to be implanted to replace the larger number of cells at the site of injury.

For this reason, dopaminergic neuron differentiated from stem cells in a 3D scaffold needs to be implanted to mimic the actual cellular microenvironment and damaged tissue site [133]. These 3D scaffolds should have microporous structure to act as the carrier for the transplanted cells and growth factor for differentiation. Pre-engineering living three-dimensional (3-D) neural tissue outside the body with controlled neuroanatomical and functional characteristics promote neuro-regeneration which can be used for the therapies of neurodegenerative diseases.

4.1 Neural tissue engineering using stem cells

Neural tissue engineering offers enormous promise in replacing damaged neural tissue and restoring the lost function of the nervous system by implantation in the form of graft or scaffold in both Central Nervous System (CNS) and Peripheral Nervous System (PNS). The CNS consists of the brain and the spinal cord, while the PNS consists of nerves that originate from the brain and spinal cord and innervate the rest of the body [134]. Tissue engineering for the peripheral nervous system are focused on axonal regeneration inside nerve graft and for the central nervous system are focused on cell transplantation and electrical stimulation by using cell culture techniques and biomaterials [134].

MSC is isolated from bone marrow, adipose tissue, umbilical cord and other tissues. MSC collected from bone marrow are also capable of differentiating into neuronal cells on tissue engineered nanofibrous scaffolds [76]. The combination of mesenchymal stem cells and

biomaterial scaffolds offers a hopeful strategy for engineering functional tissues and cellular delivery for Parkinson's disease treatment. There is an absolute need for a scaffold for stem cell transplantation therapy using stem cells, as stem cells have a tendency to migrate out of the injury site to other sections of the brain and the therapy would not be effective in that case. Table 4.1 demonstrate the benefit of mesenchymal stem cell application in treating Parkinson's disease [75].

Table 4.1: Bone-marrow derived MSC from different sources for PD treatment

MSC source	Route of MSC	Results	Ref.
Sprague-Dawley Rats	Intrastriatal	Differentiated MSCs improved rotational behavior; partial restoration of tyramine-induced DA release in the striatum	[135]
		MSCs cultured in hypoxic conditions induced an increase in striatal DA levels and behavioral improvements	[136]
	Substantia nigra	BM-MSCs differentiated and induced behavior improvements and protection of nigrostriatal system	[137]
	Intravenous	Improvements in motor behavior and protection of TH+ fibers in the striatum and SN	[138, 139]
Human	Intrastriatal	Improvements in rotation behavior, inhibition of DA depletion in the striatum; regeneration in striatal DAergic nerve terminal network	[140]

		Differentiated MSCs reduced rotational behavior Naı¨ve MSCs induced neurogenesis in the subventricular zone	[141]
	Femoral vein	Reduction in rotational behavior; increase in the number of TH+ neurons; inhibition of glial activation	[142]
	Substantia nigra	Differentiation into DAergic neurons in vivo; behavioral improvements	[143]
EGFP-Dark Agouti rats	Intranasal	Neuroprotective and anti-inflammatory role of MSCs; recovery of motor function; increased TH and DA levels in striatum and SN; decreased apoptosis	[144]
Human	Intrastriatal	Behavioral improvements	[145]
Human	Tail vein	Reduced loss of TH+ cells; increased DA levels in striatum; decreased activation of microglia and caspase-3 activity	[146]
Human	Tail vein	Decreased loss of TH+ cells in the SN and inhibition of microglia activation	[147]
Human	Intrastriatal	No suppression of inflammatory response; no neurogenesis	[148]

Wistar Rat	Carotid artery	No effects on progression of neuronal damage or on motor impairment; reduced turning behavior	[149]
	Intrastriatal	Immune response to allogeneic transplanted BMMSCs	[150]
Wistar Rat	Intravenous	Prevented loss of TH+ cells in the SN; no improvements in motor activity	[151]
Autologous	Putamen	Differentiation to A9 DAergic neuron-like cells; motor function improvements	[152]

Human MSC are known to home to various sites and even cross the BBB to the CNS to restore the levels of DA neurons. Results from the studies mentioned in Table 4.1 strongly implied the role and potential for MSC to differentiate into DA neurons [135-152].

4.2 Biomaterials as tissue engineering scaffolds

Biomaterials configured as three-dimensional (3D) scaffold hydrogels provide stem cells with an appropriate microenvironment in order to reproduce the functions of the damaged tissue [78]. Natural scaffolds such as collagen, fibrin, and hyaluronic acid are generally more biocompatible, degrade into non-toxic byproducts, and contain innate cell adhesion and signaling elements. Synthetic scaffolds such as polylacticoglycolic acid (PLGA) or polyethylene glycol (PEG) can be tuned to have ideal mechanical and chemical properties, are optimal for manufacturing purposes, but formation of toxic products during polymerization and degradation can be drawbacks. Key parameters in the design of scaffolds for stem cell transplantation are

mechanical properties, biocompatibility, polymerization and degradation rate, and adhesion site availability. It has been shown that stem cell behavior can be directed by the stiffness of the substrate in vitro [78].

The various components that comprise the Extracellular matrix (ECM) of the cells provide a robust foundation for developing scaffolds based on natural biomaterials [78]. In addition, natural materials tend to be biocompatible and contain sites for cellular adhesion, providing substrates for stem cell survival, growth, and function. Injectability of these materials allows for *in situ* polymerization in addition to the formation of a tight apposition with the lesion cavity, especially in the case of stroke [78]. Modern tissue engineering is increasingly using three-dimensional structured biomaterials in combination with stem cells as cell source, since mature cells are often not available in sufficient amounts or quality [78, 153].

The transition from traditional two-dimensional (2D) cell culture platforms toward three-dimensional (3D) systems seeks to overcome the limitations of 2D cellular models and mimic the native cellular microenvironment. Such 3D tissue culture platforms provide the opportunity for further understanding of structure−function relationships and tissue pathophysiology; as well as facilitate the development of novel regenerative medical treatments to help restore and strengthen lost functionality. A critical challenge of this evolution has been the development of biocompatible scaffolding to simulate the natural extracellular matrix (ECM). Beyond the biological materials such as protein-based ECMs, novel engineered materials offer improved functionality and customization for localized chemical delivery and bioactivity monitoring. Among these materials, graphene has become an excellent alternative because of physical, electrical, and mechanical properties [154].

In biomedical applications, 3D macroscopic structure is needed as 2D graphene often does not meet the mass and volume requirements. 3D graphene foam has high specific surface area due to the porous structure, but low mechanical strength. The powder metallurgy (Nickel) template free standing GF shows better mechanical strength. The specific surface area can be measured by measuring N adsorption-desorption by BET method with BET surface analyzer and pore size was determined by BJH method with pore size analyzer [155].

Implantation of patient specific-stem cell-derived dopaminergic (DA) neurons and their regenerative responses might provide a path to functional recovery in neurodegenerative disease and brain injury [156]. The value of a lab created DA neuronal tissue in a dish using a patient's own stem cells is immense, including in vitro modeling and regenerative medicine [157]. First, tissues created from the patient's own mesenchymal stem cells can be potentially transplanted back without ethical or immunological challenges [157, 158]. Second such tissue on a dish models can serve as better platforms for clinical drug testing generally performed in animals, which sometimes have drastically different outcomes compared to clinical trials [158]. In addition, a lab created tissue on a dish that accurately mimics actual brain tissue would be significant for researching not only the effect of drugs but neurodegenerative disorders like Parkinson's, Alzheimer's and ALS (Amyotrophic Lateral Sclerosis) as well [8, 159-164]. So, our long-term goal is to culture 3D, DA-neuronal tissues on a dish that can capture in vivo neuronal functions and can be useful as tissue-on-a-chip for drug cytotoxicity studies. At the same time, we are interested in providing an optimal 3D scaffold for evaluating the adhesion, culture, and differentiation of mesenchymal stem cells into DA neurons, for use as a platform for neural tissue engineering applications, such as for the treatment for neurodegenerative disorders.

4.3 MSC differentiation into DA neuron in 3D graphene scaffold

Biomimetic 3D scaffolds are preferred tools for culturing neurons as they provide defined mechanical and physicochemical properties with an interconnected porous structure that can enable a higher or more complex organization than traditional two-dimensional monolayer conditions [165]. Changes in the internal geometry and mechanical properties of such 3D scaffolds can impact cell behavior including survival, growth, and cell fate choice [165]. Other specific characteristics required of scaffolds for culturing neurons are electro-conductivity and nano-architecture, both of which are offered by Graphene [60, 166]. Graphene is composed of a single layer of carbon atoms arranged in a two-dimensional honeycomb lattice [167]. Other than being routinely used for electrical, optical and thermal applications, studies also proposed the potential of graphene for biomedical applications [167]. Graphene can be used as an optimized scaffold for cell-culture, tissue engineering, and regenerative medicine applications [60]. Published works of others have shown that graphene substrates can support the adhesion, proliferation and differentiation of mesenchymal stem cells (MSC), induced pluripotent stem cells (iPSC), and other mammalian cells [60]. Specifically for neural tissue regeneration, graphene has demonstrated the ability to perform as an effective platform compatible with neural cells or their precursors [60], and promoted neurogenesis, as assessed by neurite sprouting and neural network formation [166, 168]. Human MSC growth, followed by neural differentiation was also supported by a monolayer of graphene substrate [169]. Further, the capability of graphene substrates to electrically stimulate differentiated neuronal cells was demonstrated [170]. Our recent published work showed that Graphene-oxide coatings enhanced the survival and proliferation of SH5YSY neuronal cells [59].

Based on these reports, we hypothesized that Graphene-based substrates may be a promising scaffold material for neural tissue engineering. In this study, our objective was to utilize

a commercially available 3D Graphene scaffold termed as ‘Graphene foam’ (GF) for culturing mouse MSC and differentiating them into DA neurons. We hypothesized that these MSC-differentiated DA neurons when cultured in a 3D scaffold, will more closely exhibit morphologies, functions and other necessary characteristics of in vivo DA neuronal tissues, compared to 2D culture or monolayer substrates. To culture cells on the hydrophobic Graphene substrates [125], they need to be coated with proteins, such as Laminin [154, 171] to promote hydrophilicity and cell adhesion onto these surfaces. On the other hand, collagen coating is a well-established procedure for cell culture and collagen coatings when applied to Graphene-based substrates were shown to not interfere with the porous structure of Graphene [172]. So, we opted to coat the hydrophobic graphene-foams using collagen as it would lead to the formation of a hydrophilic, porous and conductive scaffold ideal for neuron culture.

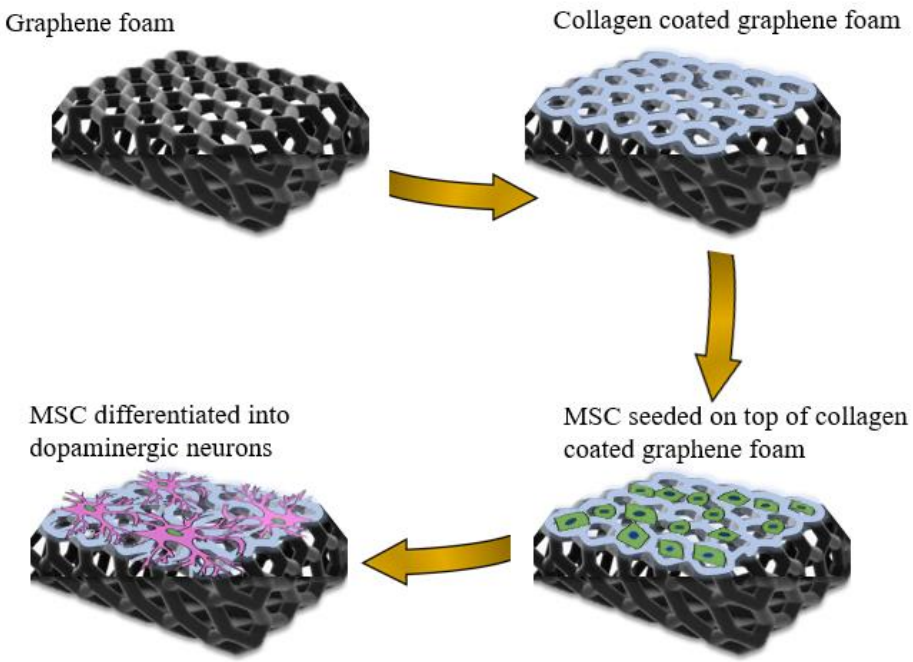

Figure 4.2: Mesenchymal stem cell (MSC) was differentiated into dopaminergic (DA) neuron on top of collagen coated graphene foam scaffold

Figure 4.2 shows the steps that we followed to fabricate the 3D graphene scaffold to differentiate MSC into DA neurons. This work will significantly contribute by enabling a platform that will allow us to study interactions between healthy DA neurons, their synaptic communications, and identify mechanisms involved in DA neuron apoptosis during injury and disease. As studying DA neuronal cell death in human brains is extremely difficult and invasive, development of such in vitro 3D models of DA neurons would make it feasible to probe cellular and molecular mechanisms of neurodegenerative disorders and implement novel therapeutic strategies. This study is innovative as the technique might be adaptable for engineering other 3D tissue models from different stem cell types.

4.3.1 Preparation of the graphene-foam and collagen coating

3D Multilayer Freestanding Graphene Foams (GF) (2″ X 2″) were purchased from Graphene Supermarket (Calverton, NY). For cleaning, these foams were washed with 70% ethanol, followed by UV exposure for 30 min in a laminar sterile flow hood. Using a sterile biopsy punch (~1 mm deep, 8 mm diameter) samples were prepared for further processing and experimentation. These pristine GF discs were collagen coated [173] and crosslinked with genipin [174], using published guidelines. For coating of the GF, collagen from Bovine Achilles Tendon (Sigma-Aldrich) at a concentration of 9 mg/ml in 0.2 M acetic acid was used for extraction of acid-soluble collagen (for 24 hr @ 200 rpm). The extract was analyzed using Fourier Transform Infrared Spectroscopy (FTIR) to confirm the presence of collagen, in comparison with existing literature.

After collagen coating, GF samples were incubated at 37°C for 24 hr in Genipin (stock solution of 100 mM in DMSO, Enzo Life Sciences), prepared using a ratio of 1:100 of Genipin in

1X PBS to further crosslink the collagen atop the GF [175]. After 24 hr, the crosslinked collagen coated GF samples were washed using sterile 1X PBS (Sigma-Aldrich) for 3 times prior to consecutive experiments.

To confirm the crosslinking of the collagen using Genipin atop the GF using the procedure described above [175], rheometry was used to compare the properties of the non-crosslinked versus the crosslinked collagen samples. Collagen gels for rheometry were formed as described previously [176] and cut using a biopsy punch (~1 mm deep, 8 mm diameter). The gels were pre-swollen in 1X PBS before testing. Oscillatory shear stress rheometry was performed (1% strain, 0.5 – 50 Hz) using an Anton-Paar MCR101 rheometer (Anton-Paar, Graz, Austria) with an 8 mm parallel plate geometry. The strain and frequency range were analyzed within the linear viscoelastic range of the gels by frequency sweeps. Elastic modulus was calculated through complex shear modulus with storage and loss modulus, and complex viscosity was measured at 1.76 - 1.99 Hz for all samples, as done earlier [176].

4.3.2 Experimental analysis

Scanning Electron Microscopy (SEM)

Images of the surfaces of the pristine GF were acquired using SEM (S-4800, Hitachi, Japan) at voltages of 10 kV. For imaging of the collagen-coated GF, samples were air-dried and coated with Graphite Spray (Electron Microscopy Sciences, Hatfield, PA) to minimize charging during observation and imaged at voltages of 1 kV.

Raman Analysis

The pristine GF and collagen-coated GF was characterized by Raman spectroscopy to study the vibrational properties of the material to provide information on molecular vibrations and crystal structures.

X-Ray Diffraction Analysis

For the phase analysis, the samples were air-dried prior to X-ray diffraction (XRD, D8 Discover, Bruker's diffractometer, Karlsruhe, Germany). XRD was carried out at 40 kV voltage and 40 mA currents with CuKα wavelength (1.54056 Å) and 2θ ranges from 10° to 50° at a scanning rate of 3°/min with a step size of 0.1°.

Electrical characterization

To explore the electrical transport properties of GF and collagen-coated GF, a two-probe measurement was conducted using a Micromanipulator (Carson City, Nevada). In the measurements, tungsten probes were used to measure the I-V (Current vs. Voltage) curve when a bias voltage of 0 to 3 V was applied.

Biocompatibility testing

Strain C57BL/6 Mouse Mesenchymal Stem Cells (mouse MSC, catalog #: MUBMX-01001) and Mouse Mesenchymal Stem Cell Growth Medium (complete growth medium, catalog #: MUXMX-90011) were purchased from Cyagen (Santa Clara, CA, USA). The cells were grown and stabilized for at least 8 passages before being used in further experiments. Prior to being introduced into the 3D scaffolds, cells were labeled with PKH26 red fluorescent dye (Sigma) following manufacturer's protocols. These labeled mouse MSC were seeded atop collagen coated-GF, or controls (tissue culture plastic wells) in a density of 1 X 10^6 cells/ml placed within 24 wells of a tissue culture well plate (Fisher-Scientific) and cultured for at least 72 hr (37°C, 5% CO_2). Confirmation of cell retention within the collagen coated-GF was done using SEM (as described before) and inverted confocal fluorescence microscopy (ZEISS LSM 700 Confocal, Germany).

Flow Cytometry (FACS) analysis

To estimate cell proliferation and overall biocompatibility of the collagen coated-GF, mouse MSC were pre-stained using Cell Trace Violet, proliferation kit (Invitrogen, Carlsbad, CA, USA) using manufacturer's protocols. These pre-stained cells were seeded (4 X 10^6 cells/ml) atop 3D collagen coated-GF, 2D tissue culture plastic wells (controls) and cultured for 24 hr, and 48 hr respectively (37°C, 5% CO_2). After 24- and 48-hr, samples were treated using Trypsin-EDTA (0.25%, phenol red) (ThermoFisher, Waltham, MA), cells were detached, extracted and processed for flow cytometry (FACS). Extracted cells were fixed and processed further for FACS (Beckman Coulter Gallios Flow Cytometer, Brea, CA, USA) using excitation and emission wavelengths of 405 and 450 nm respectively. Pre-stained cells grown in plastic Petri dishes for 72 hr served as positive controls. Negative controls included non-stained cells cultured on plastic Petri dishes for 72 hr.

Differentiation of mouse MSC into DA neurons

Mouse MSC used for the differentiation were cultured and passaged as described below. Prior to cell seeding, T-75 culture flasks were coated with 0.1% gelatin (Sigma Aldrich, St. Louis, MO, USA) and incubated (37°C for 1 hr). After this, the cell suspension in complete culture medium was transferred to a gelatin-coated T-75 flask and incubated for 1 hr (37°C, 5% CO_2 and 95% RH). Prior to cell culture, the gelatin solution used for coating of the flasks was aspirated. After 70% confluency in culture was attained, cells were trypsinized and passaged for further experiments.

For induction of differentiation of mouse MSC into DA neurons, 2 types of 3D scaffolds were used. These included the collagen coated-GF and collagen gels only. For the preparation of collagen gels, the collagen extract was loaded into a 10 ml syringe (BD Biosciences, San Jose,

CA) and ejected into a 24 well for deposition and settling. Once a smooth surface of the deposited collagen was observed, the wells were incubated with the genipin solution for crosslinking (as described earlier). After crosslinking was completed, uniform size disc-shaped samples for both collagen coated-GF and collagen gels only were punched out using a biopsy punch (~1 mm deep, 8 mm diameter).

For the differentiation of mouse MSC into DA neurons atop 3D scaffolds or 2D culture plastic, published protocols were followed [177]. For the differentiation, initial cell seeding density of mouse MSC in the 2D plastic wells was maintained at 3 X 10^5 cells/ml based on published guidelines [58], and for the 3D scaffolds, cell density was adjusted based on the total volume of the scaffolds (6 X 10^6 cells/ml). Briefly, passaged mouse MSC cells were seeded on poly-D-lysine (BD Biosciences) coated dishes (using complete growth media for mouse MSC) and after 24 hr the culture medium was replaced using Neurobasal Media (Catalog number: 21103049; Thermo Fisher-Scientific). At this point, Sonic hedgehog (SHH, R & D Systems, Minneapolis, MI), Fibroblast growth factor (FGF8, R & D Systems), Basic fibroblast growth factor (BFGF, R & D Systems) were added and incubated for 6 days. After this, Brain-derived neurotrophic factor (BDNF, Cell Sciences, Canton, MA) was added to the culture and further incubated for 3 days. After a total of 9 days of culture, to confirm the differentiation of MSC into DA neurons, the cell-seeded scaffolds and controls were fixed with 4% paraformaldehyde (Sigma) for 15 min (25°C) and then permeabilized with 0.2% Triton X-100/PBS for 1 hr. After blocking with 1% normal goat serum (NGS/PBS, Sigma) for 1 hr at room temperature, the samples were incubated with a mouse monoclonal antibody to β-III tubulin [5.2F] for location of β-III Tubulin and for detection of Vimentin, the samples were incubated with Vimentin mouse monoclonal antibody (24 hr at 4°C) followed by a goat polyclonal secondary antibody to mouse IgG1-heavy chain (FITC) (Abcam,

Cambridge, UK) (2 hr at 25°C). For detection of TH, the samples were incubated with a purified rabbit monoclonal IgG antibody to TH and for detection of NeuN, the samples were incubated with NeuN rabbit polyoclonal antibody (24 hr at 4°C) followed by a goat anti-rabbit IgG secondary antibody, Alexa Fluor 488 conjugate (2 hr at 25°C) at a dilution of 1:1000 for in the dark. The samples were then washed with 1X PBS thrice and mounted using Fluoromount-G with DAPI (Thermo Fisher-Scientific) and imaged using a confocal fluorescence microscopy (Olympus IX81 inverted fluorescence motorized microscope, Japan).

As a control, for the differentiation of mouse MSC into DA neurons, we chose to induce differentiation in human MSC alongside (online supplement) the mouse MSC. This was important to confirm the validity of the differentiation induction protocol in mouse MSC, compared to the human MSC and also contrast the response of both cell types to the same differentiation protocol.

Axonal extensions on proximal and distal sides of differentiated neurons in collagen coated-GF and in collagen was measured by calculating the axonal outgrowth length, visualized with β-III tubulin or NeuN and analyzed using ImageJ software [178]. Final results were expressed as average length of neurite extensions in collagen coated-GF and in collagen, normalized with controls (cells differentiated in 2D wells).

Statistical analysis: All samples were present in triplicate unless otherwise mentioned. Numerical data are expressed as the mean ± standard deviation. Microsoft Excel Student's t-test was performed to determine if the averages of any two sample datasets compared were significantly different. p-values less than 0.05 were considered significant.

4.4 Results and Discussion

As shown in Figure 4.3 A, the pristine GF was extremely light, hydrophobic and fragile during routine handling. For this reason, the pristine foams had to be coated with collagen to retain hydrophilicity, increase their weight and improve their handling characteristics (Figure 4.3 B, C).

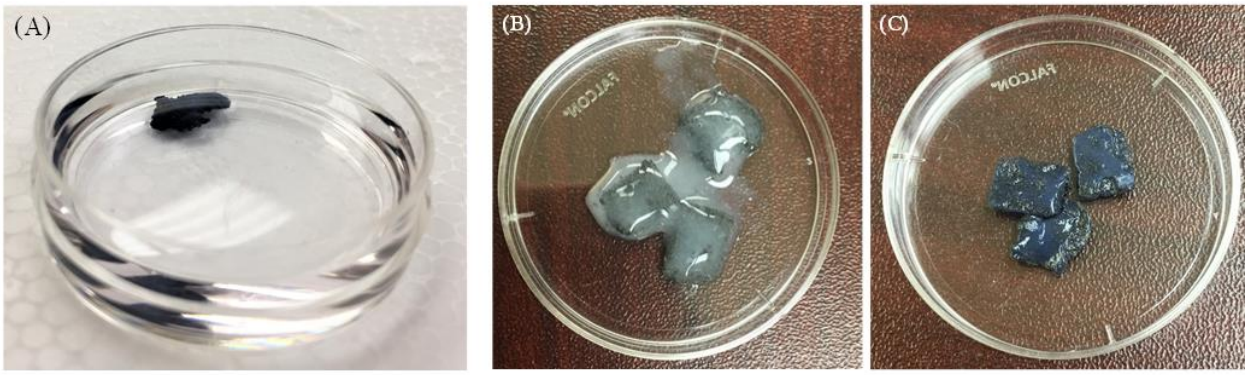

Figure 4.3: (A) Pristine Graphene foam floating in PBS in a 60 X 15 mm Petri dish. (B) Graphene foam being coated with Collagen. (C) Graphene foam after Collagen coating was crosslinked with Genipin (100 X 15 mm Petri dish shown in (B) and (C)).

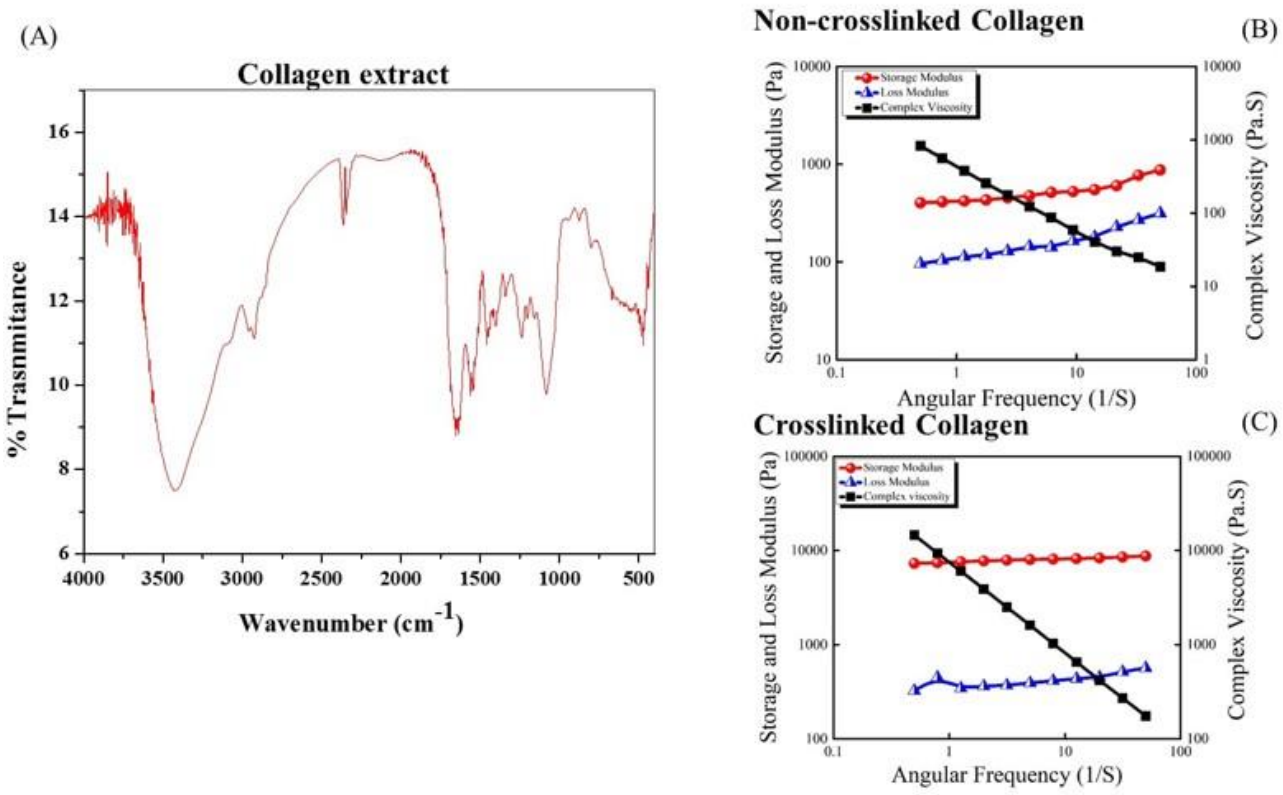

Figure 4.4: (A) FTIR spectra of collagen extract. Shown in (B) and (C) are Rheology analysis of the non-crosslinked and crosslinked collagen, respectively. Characteristic datasets were obtained from disc shaped (8 mm) samples of collagen, in both cases.

The FTIR spectra of acid soluble collagen extract are shown in Figure 4.4 A. A free N-H stretching vibration was evident in the range of 3400–3440 cm^{-1}. The hydrogen bonding of the N-H group of the peptide was evident at 3300 cm^{-1} [179]. The amide-I band was evident around 1650 cm^{-1}, fitting well the range of 1625–1690 cm^{-1} for general amide-I bands position. The amide-II band was detected around 1540 cm^{-1}, compared to the normal absorption range of the amide-II bands position (1550–1600 cm^{-1}). This was due to the existence of hydrogen bonds in collagen [179]. The helical structure of the collagen was confirmed from IR absorption ratio between 1235 (amide-III) and 1450 bands, which was approximately equal to each preparation. The results showed the helical structure of collagens were kept well. In addition, a strong C-H stretching vibration was evident at 2854 cm^{-1} and at 1745 cm^{-1}.

It was essential to confirm the crosslinking of the collagen atop the GF by a secondary technique, other than by visual confirmation (Figure 4.3 C). Therefore, rheometric analysis of the non-crosslinked and crosslinked collagen samples was done, from which it was determined that the strain and frequency range were within the linear viscoelastic range of the gels by amplitude and frequency sweeps (Figure 4.4 B, C). We were able to generate crosslinked gels of significantly enhanced elastic modulus ~ 5.0 KPa compared to the non-crosslinked samples which revealed an elastic modulus ~ 1.78 KPa. Additionally, crosslinking increased the complex viscosity of the gels from 277–2610 Pa-s.

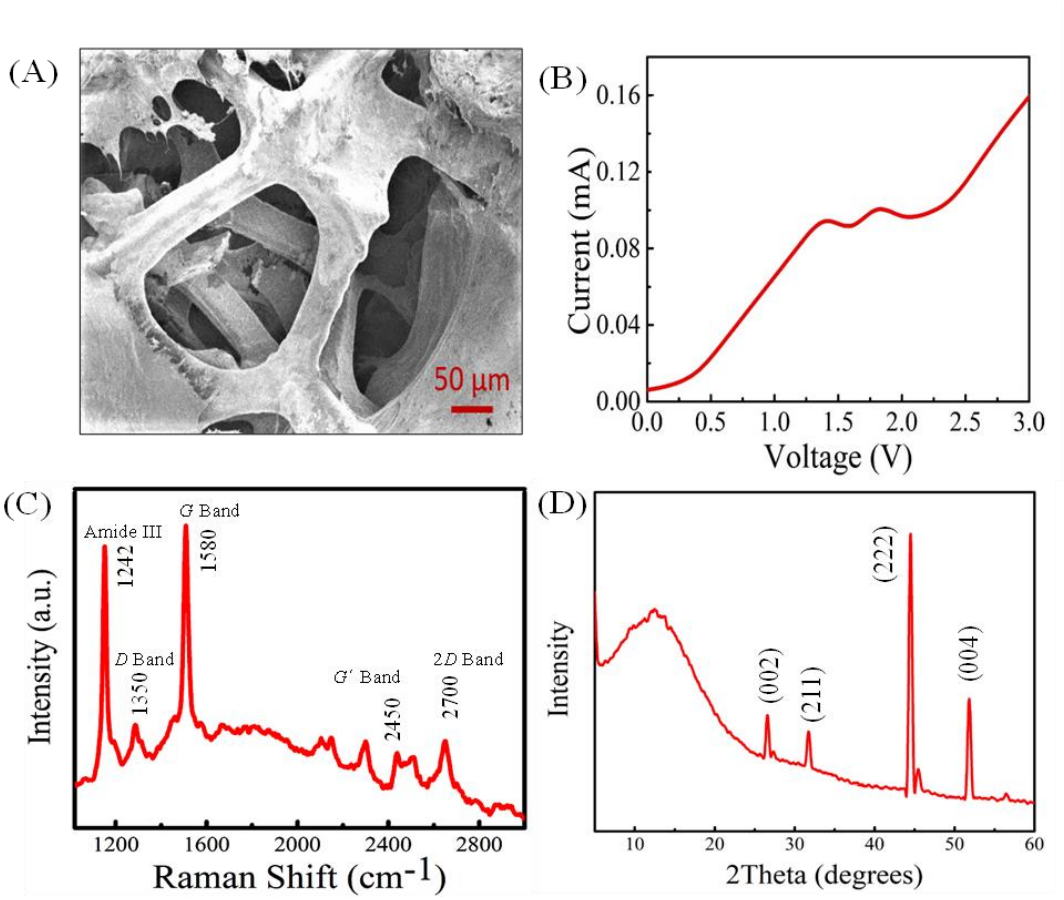

Figure 4.5: Material characterization of Graphene foam, coated with Collagen coating and crosslinked with Genipin. (A) Scanning Electron Microscopy (SEM). (B) Current Voltage (I-V) characteristics. (C) Raman and (D) XRD spectra, respectively.

Figure 4.5 A showed a characteristic SEM image of a collagen coated-GF that confirmed the deposited collagen coating, in comparison with the pristine GF. Further, it was evident that the collagen coating did not alter the basic morphology and architecture of the GF. From the I-V (current vs. voltage) curve, it is clear that the GF exhibits a non-linear behavior with current level of ~ 0.10 A at 3 V, while the collagen-coated GF also exhibited a non-linear behavior but with three orders of magnitude drop in current (~ 0.16 mA at 3 V) in Figure 4.5 B. For the collagen-coated GF, the curve did not appear as smooth as the GF, as collagen is an insulator by nature which introduces noise to the signal. From this measurement, it is clear that the collagen-coated GF yields reasonable electrical transport compared to pristine GF which paves the way for further electric stimulation of neuronal cells.

Figure 4.5 C demonstrates the typical Raman spectra of a collagen coated-GF using a 532 nm laser at room temperature. The Raman spectra of the 3D GF contained two major peaks near 1580 and 2700 cm^{-1}, corresponding to the *G* and *2D* bands of graphene. There is no major *D* band in the Raman spectra of the pristine GF, which confirmed that it is almost defect-free. The integrated intensity ratio of the *G* to *2D* band (*G*/*2D*) indicates that the GF was primarily multilayered graphene [180]. After coating the GF with collagen, *D* peak appeared near 1350 cm^{-1} and some other peaks emerged including a minor peak at ~ 2,450 cm^{-1} (*G′* band). The defect was increased from 0.02 to 0.7 in collagen-coated GF which is estimated from the intensity ratio of the *D* band and *G* band (*D*/*G*) [181]. The amide-III peak appeared at 1242 cm^{-1} which is a characteristic

of the collagen (Figure 4.5 C), though the amide-I and amide-II peaks were absent in the spectra [182]. These results confirmed the successful deposition of collagen atop 3D GF.

XRD spectra of the collagen-coated GF is shown in Figure 4.5 D. The two diffraction peaks at $2\theta = 26.5°$ and $2\theta = 55°$ correspond to the (002) and (004) planes of graphene respectively where, the intensity of the peak at $2\theta = 26.5°$ got reduced for the collagen coating [181, 183]. The diffraction peaks of collagen appeared corresponding to the crystallographic planes (211) and (222) at about $2\theta = 32°$ and $2\theta = 45.3°$ indicating traditional mineralized collagen [184].

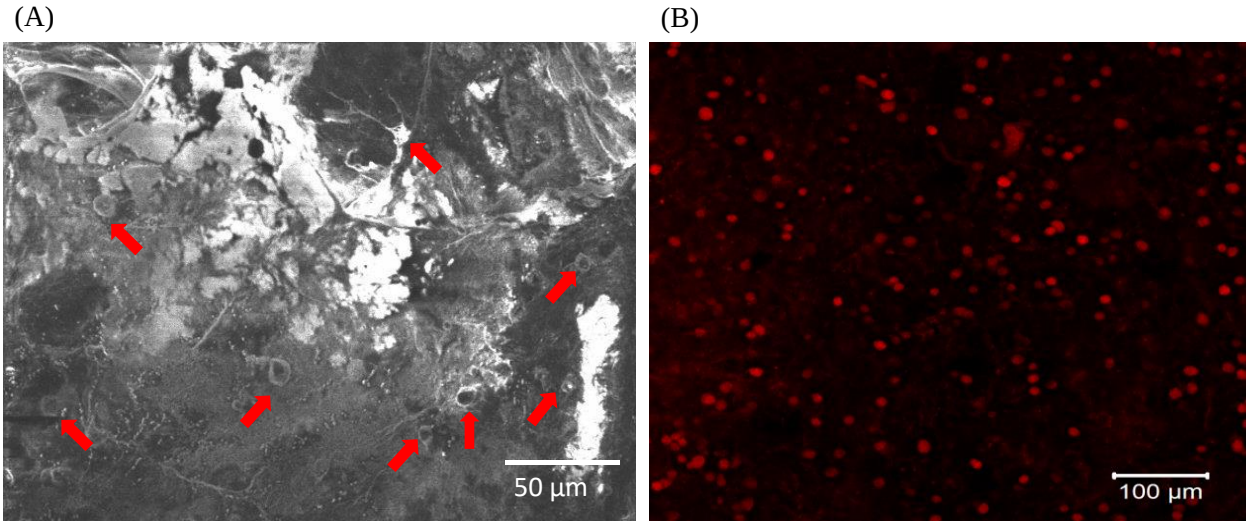

Figure 4.6: Adhesion and Retention of mesenchymal stem cells cultured in collagen coated-GF shown by (A) SEM imaging and (B) Fluorescent images of PKH26 pre-stained cells within the scaffold. Red arrows in (A) point to the cells and their extension processes.

Figure 4.6 confirmed the retention of mouse MSC within the collagen-coated GF after a sustained in-vitro culture period. The cells appeared to grow homogenously throughout the entire culture area and appeared to exhibit extensions to connect and network with the substrate (Figure

4.6 A, depicted by red block arrows). This observation was confirmed by the evidence of pre-stained cells retained within the collagen-coated GF (Figure 4.6 B).

.

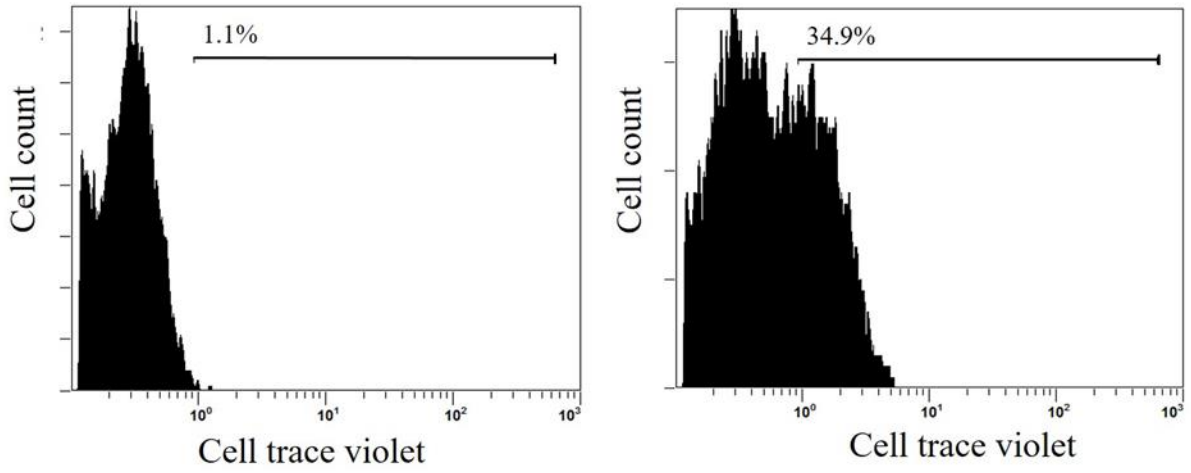

Figure 4.7: Viability and proliferation of mesenchymal stem cells in collagen coated-GF by FACS analysis. Cells pre-stained with cell trace violet were cultured upto (A) 24 hr. and (B) 48 hr. within collagen coated-GF.

Results from FACS analysis (Figure 4.7) showed that after 24 hr of culture, 1.1% of the total number of cells seeded had proliferated in comparison to controls (unstained, 0.3%). After 48 hr of culture, 34.9% of the cells were found to have proliferated (in comparison with 32% proliferating cell population in positive controls). Further, the occurrence of multiple peaks (Figure 4.7 B) revealed the presence of consecutive proliferating generations of cells, confirming that the GF was not cytotoxic and promoted mouse MSC adhesion and growth

For the first time in this study, we adopted and optimized a differentiation protocol for induction of DA neuronal differentiation of mouse MSC based on others published protocols using human MSC [177]. We succeeded in reducing the overall differentiation protocol duration from

12 days to 9 days in mouse MSC, compared with human MSC. This would allow results to be achieved rapidly compared to previously reported literature [177].

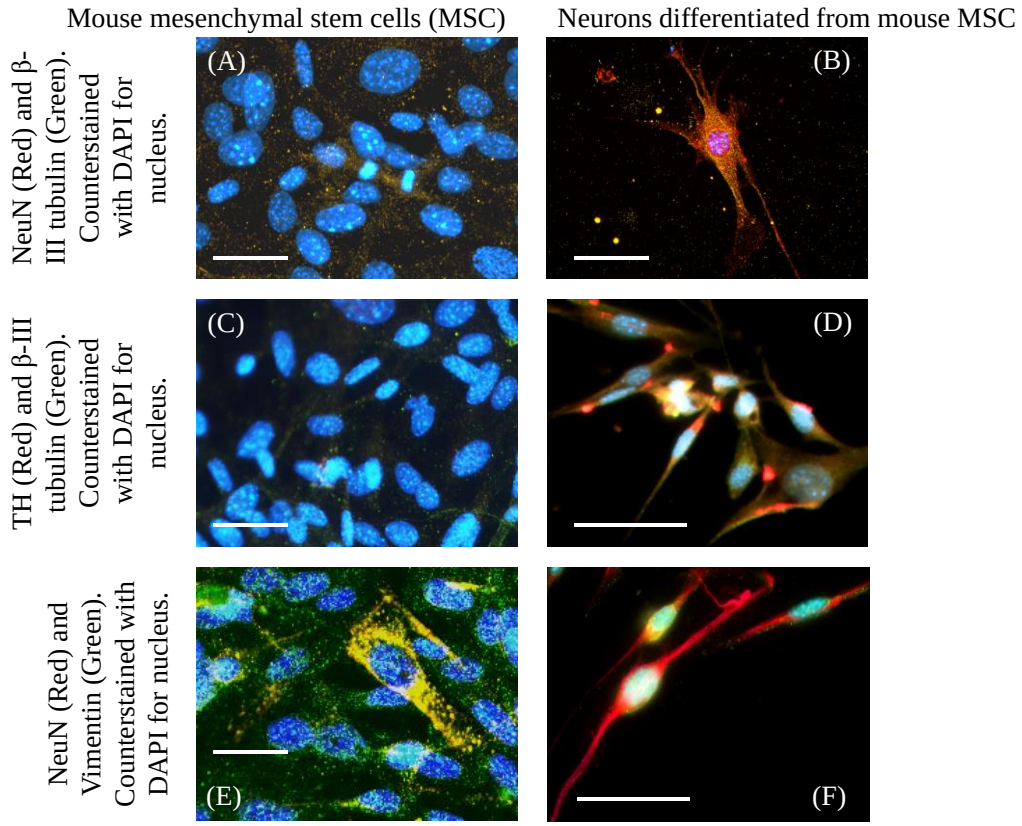

Figure 4.8: Confirmation of differentiation of mouse mesenchymal stem cells (MSC) into a neuronal phenotype as they stained positively for (B) β-III tubulin and NeuN. These differentiated neurons exhibited a phenotype resembling DA neurons as they positively stained for (D) Tyrosine Hydroxylase (TH) and β-III tubulin. Further these differentiated DA neurons did not stain positively for (F) Vimentin. Controls consisting of undifferentiated mouse MSC did not stain positively for (A) NeuN and β-III tubulin and (C) TH and β-III tubulin. But they stained positively for (E) Vimentin. Scale bar is 100 µm in all images.

The confirmation of differentiation of mouse MSC into neurons, stained by the neuronal markers, β-III Tubulin [185] and NeuN [186], was clearly evident (Figure 4.8 B, F) by atypical

neuronal cell-like morphology and extensions, in comparison with controls (Figure 4.8 A, E). It should also be noted that these differentiated neurons expressed a phenotype resembling DA neurons due to their positive expression and enhanced levels of TH [187], unlike their undifferentiated controls (Figure 4.8 C and D). Although the undifferentiated mouse MSC did not express neuron like morphology or neuronal markers (Figure 4.8 A, C, E), but stained positively for Vimentin, a stem cell marker [188]. These results collectively confirmed the differentiation of mouse MSC into DA neurons.

A comparison of the morphology and expression of and neuronal and dopamine producing markers in neurons differentiated in both collagen coated-GF and collagen gels, revealed significant differences (Figure 4.9). Cells in contact with the collagen coated-GF not only showed enhanced expression of both neuronal markers, β-III Tubulin and NeuN (Figure 4.9 B, D, F) but also TH (Figure 4.9 D) in comparison with cells in contact with collagen gels ((Figure 4.9 A, C, E). Comparison of normalized average neurite extension from cells differentiated in both collagen coated-GF and collagen revealed significant differences ($p = 0.002$) (Figure 4.10). This result implies that the 3D GF might be a better substrate for neuronal culture compared with collagen gels. The images of the neuronal extensions within the 3D scaffolds corresponded to others published images of neuronal networks [189].

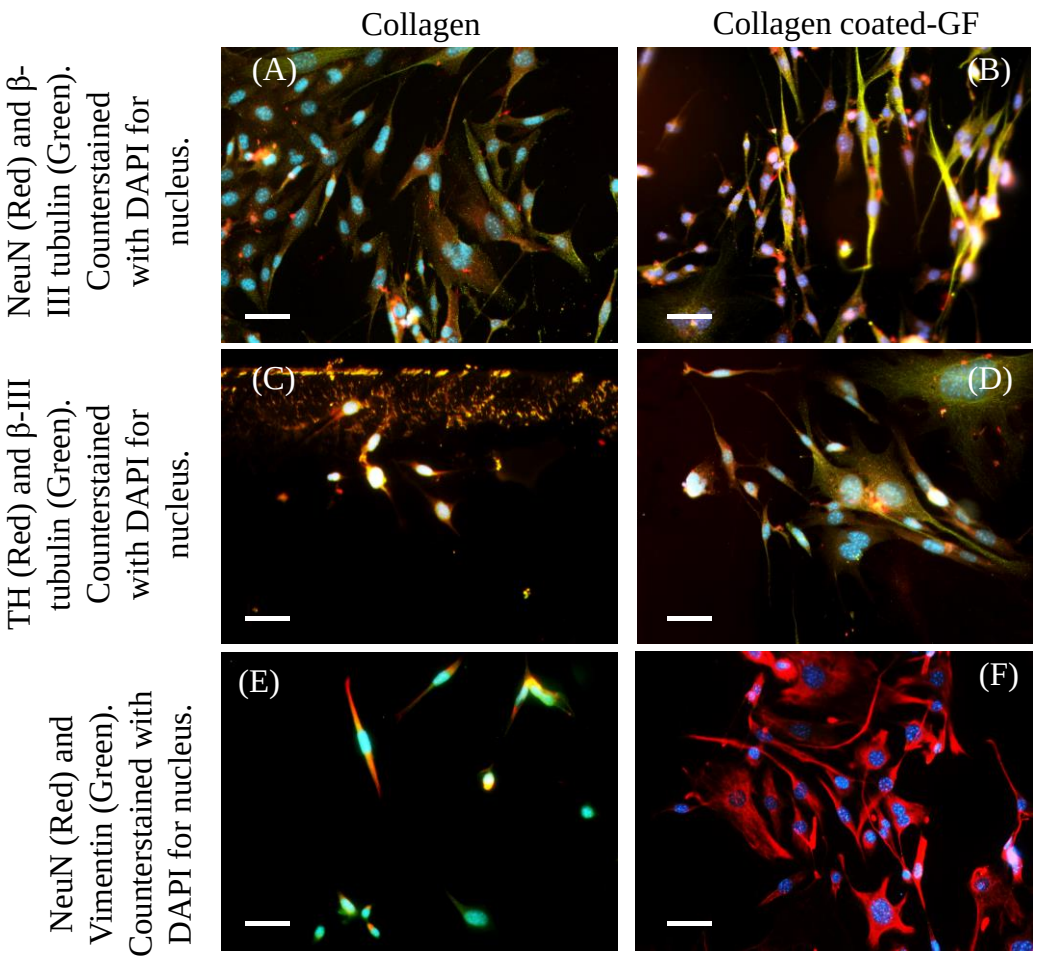

Figure 4.9: Comparison of differentiated DA neurons from mouse MSC in contact with (A), (C), (E) collagen gels and in contact with (B), (D), (F) collagen coated-GF. Confirmation of differentiation of mouse mesenchymal stem cells (MSC) into a neuronal phenotype resembling DA neurons was exhibited in all cases but, cells differentiated in Graphene foam-based scaffolds exhibited significantly longer neurite extensions than those cultured in contact with collagen. Scale bar is 30 μm in all images.

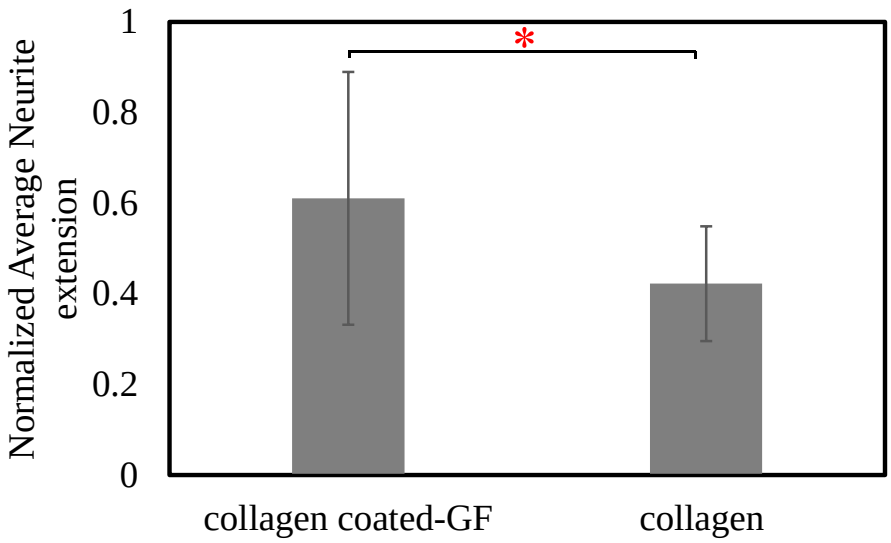

Figure 4.10: Comparison of normalized average neurite extension length between cells differentiated in collagen coated-GF and collagen only. ∗ Indicates difference between the plotted values were statistically significant.

Although monolayer Graphene substrates have been used for MSC culture [169], it is the GF that offers a 3D porous substrate for neural cell culture and neural regeneration as also shown by other's work [190]. After coating the GF with collagen, this hybrid scaffold poses as a biocompatible, porous substrate which is effective for cell culture and differentiation. Although several types of polymer enriched GF have been fabricated [191], this is the first time GF coated with collagen was prepared and used for neural tissue engineering applications. In the future, specific growth factors could be encapsulated within these scaffolds for delivery to cultured cells for their growth or targeted differentiation [192]. As the 3D GF allows the DA neurons to maintain their morphology and function, we envision that this neuron filled scaffold can be directly implanted in vivo or be used for studies exploring neuronal functions in vitro, in the future.

4.5 Conclusions

Networks of neurons (in vivo) develop via an elaborate succession of cellular events that, when disrupted, can lead to neuron dysfunction and degeneration [84, 157, 161, 163, 170, 193-202]. Injuries or disease conditions, either in the peripheral (PNS) or central (CNS), require reconstruction through advanced regenerative medicine and/or tissue engineering approaches. In this study, our goal was to prepare a 3D scaffold suitable for MSC adhesion, growth and differentiation into DA neurons. We successfully prepared collagen coated-GF as 3D scaffolds for cell culture and differentiation. The collagen coating did not alter the basic properties of the GF but enhanced its hydrophilicity and handling characteristics at the same time. Mouse MSC adhered and proliferated well within these scaffolds. Furthermore, these MSCs were efficiently differentiated into DA neurons when seeded within these collagen coated-GF.

The outcomes from this study are both novel and significant because it will help reveal interactions between healthy DA neurons and their synaptic communications. It can also help predict mechanisms involved in injury- or disease-induced DA neuron apoptosis. Outcomes from this study can be extended to model other networks of neurons, such as cortical neurons to study normal and abnormal corticogenesis in the CNS [199], peripheral nerves that are involved in spinal cord injuries [203] or even used to model diabetic neuropathy in vitro [204].

Chapter 5: Future outlook

In this study, both materials-based and tissue engineering approaches for PD treatment was applied. In the first experiment, GO coated 316L SS surfaces did not exhibit in vitro neurotoxicity for SHSY-5Y cells and reduced their ROS expression, confirming its biocompatibility. Further, GO coatings were found to be stable and non-reactive. In SEM images, we observed surface roughness to the implant surfaces which permitted cell adhesion, spreading and proliferation, without inclusion of any additional neuronal growth factors [96]. To make the coating uniform, enhanced coating techniques can be applied such as, spin coating [205] or electrophoretic deposition [39]. The procedure employed for making GO-coatings in this study is simple, inexpensive and less time consuming.

In the second experiment, for differentiating MSC in three-dimensional graphene foam scaffolds into DA neurons collagen coating has been used to enhance the handling strength of graphene foam for cell culture convenience. Cell adhesion, proliferation and maintenance was examined by fluorescence microscopy, flow cytometry and electrical stimulation. Material characterization of the commercially available graphene foam and collagen coated graphene foam was compared by SEM, Raman spectrometry and electrical conductivity test. These studies will help develop neural tissue engineered therapies to improve clinical treatments for neurodegenerative diseases like Parkinson' disease. As mentioned earlier that DA neurons are degenerated and lost in case of PD, so cell replacement therapy is an ideal therapeutic approach for this. Stem cells can be transplanted in the central nervous system and it depends on the cell type and cell delivery method. Some researchers used poly(N-isopropylacrylamide) (pNIPAM) hydrogel to facilitate manipulation of neurons which increased the number of viable transplanted cells in rat hippocampus [206]. In some studies, fibrin gel has been used as an excellent biocompatible and injectable scaffold and cell carrier promoting cell viability and tissue regeneration [207].

The transition from traditional 2D cell culture platforms toward 3D systems seeks to overcome the limitations of 2D cellular models and mimic the native cellular microenvironment. Such 3D tissue culture platforms provide the opportunity for further understanding of structure−function relationships and tissue pathophysiology; as well as facilitate the development of novel regenerative medical treatments to help restore and strengthen lost functionality [154]. A critical challenge of this evolution has been the development of biocompatible scaffolding to simulate the natural extracellular matrix (ECM). Beyond the biological materials such as protein-based ECMs, novel engineered materials offer improved functionality and customization for localized chemical delivery and bioactivity monitoring. Among these materials, graphene has become an excellent alternative because of physical, electrical, and mechanical properties.

In biomedical applications, 3D macroscopic structure is needed as 2D graphene often does not meet the mass and volume requirements. 3D graphene foam has high specific surface area due to the porous structure, but low mechanical strength [155]. Future studies should emphasize on chemically immobilizing the growth factors directly in the GF scaffold so that it would avoid repeated surgery to deliver the healthy neurons in the brain, derived from patient's own stem cell. Mesenchymal Stem Cells have the potential to be differentiated into other tissues and also into neurons. This has generated great interest about the potential use of MSC for the treatment of degenerative diseases of the nervous system. Surface chemistry plays an important role for the adhesion of cells. Biocompatibility of graphene and GO is also important with the use of collagen.

In conclusion, engineering substrates to induce desired cell phenotype and genotype is an important strategy of scaffold design for tissue-engineering applications. Graphene can be used to enhance cell adhesion and proliferation of MSCs, and it exhibits a neuro-inductive effect via spontaneous cell polarization. Graphene films are found to be highly supportive of MSCs growth and have significant effects on cell morphology, cytoskeletal and nuclear elongation of MSCs [86]. Graphene based 3D scaffold may be a viable platform for neural tissue-engineering applications and can be used for the research of therapeutic approaches for PD and other neurodegenerative diseases.

References

[1] O. Lindvall and R. McKay, "Brain repair by cell replacement and regeneration," *Proceedings of the National Academy of Sciences,* vol. 100, pp. 7430-7431, 2003.

[2] J. T. Coyle and P. Puttfarcken, "Oxidative stress, glutamate, and neurodegenerative disorders," *Science,* vol. 262, pp. 689-695, 1993.

[3] X. Chen and W. Pan, "The treatment strategies for neurodegenerative diseases by integrative medicine," *Integrative Medicine International,* vol. 1, pp. 223-225, 2014.

[4] D. Houghton, H. Hurtig, S. Metz, and M. Brandabur, *Parkinson's disease: medications*: National Parkinson Foundation, Incorporated, 2008.

[5] N. Ray, N. Jenkinson, S. Wang, P. Holland, J. Brittain, C. Joint*, et al.*, "Local field potential beta activity in the subthalamic nucleus of patients with Parkinson's disease is associated with improvements in bradykinesia after dopamine and deep brain stimulation," *Experimental neurology,* vol. 213, pp. 108-113, 2008.

[6] L. J. Findley, "The economic impact of Parkinson's disease," *Parkinsonism & related disorders,* vol. 13, pp. S8-S12, 2007.

[7] S. L. Kowal, T. M. Dall, R. Chakrabarti, M. V. Storm, and A. Jain, "The current and projected economic burden of Parkinson's disease in the United States," *Movement Disorders,* vol. 28, pp. 311-318, 2013.

[8] F. Han, D. Baremberg, J. Gao, J. Duan, X. Lu, N. Zhang*, et al.*, "Development of stem cell-based therapy for Parkinson's disease," *Translational neurodegeneration,* vol. 4, p. 16, 2015.

[9] P. L. Martínez-Morales and I. Liste, "Stem cells as in vitro model of Parkinson's disease," *Stem cells international,* vol. 2012, 2012.

[10] L. I. Golbe, "Young-onset Parkinson's disease A clinical review," *Neurology,* vol. 41, pp. 168-168, 1991.

[11] L. E. Dibble, J. Christensen, D. J. Ballard, and K. B. Foreman, "Diagnosis of fall risk in Parkinson disease: an analysis of individual and collective clinical balance test interpretation," *Physical therapy,* vol. 88, pp. 323-332, 2008.

[12] J. C. Amatniek, W. A. Hauser, C. DelCastillo-Castaneda, D. M. Jacobs, K. Marder, K. Bell*, et al.*, "Incidence and predictors of seizures in patients with Alzheimer's disease," *Epilepsia,* vol. 47, pp. 867-872, 2006.

[13] R. J. Bateman, P. S. Aisen, B. De Strooper, N. C. Fox, C. A. Lemere, J. M. Ringman*, et al.*, "Autosomal-dominant Alzheimer's disease: a review and proposal for the prevention of Alzheimer's disease," *Alzheimer's research & therapy,* vol. 3, p. 1, 2011.

[14] M. Barichella, E. Cereda, and G. Pezzoli, "Major nutritional issues in the management of Parkinson's disease," *Movement disorders,* vol. 24, pp. 1881-1892, 2009.

[15] S. Johnson, "Micronutrient accumulation and depletion in schizophrenia, epilepsy, autism and Parkinson's disease?," *Medical hypotheses,* vol. 56, pp. 641-645, 2001.

[16] A. Z. Sherzai, M. Tagliati, K. Park, S. Pezeshkian, and D. Sherzai, "Micronutrients and Risk of Parkinson's Disease: A Systematic Review," *Gerontology and geriatric medicine,* vol. 2, p. 2333721416644286, 2016.

[17] K. R. Chaudhuri, D. G. Healy, and A. H. Schapira, "Non-motor symptoms of Parkinson's disease: diagnosis and management," *The Lancet Neurology,* vol. 5, pp. 235-245, 2006.

[18] H. C. Cheng, C. M. Ulane, and R. E. Burke, "Clinical progression in Parkinson disease and the neurobiology of axons," *Annals of neurology,* vol. 67, pp. 715-725, 2010.

[19] C. M. Tanner, R. Ottman, S. M. Goldman, J. Ellenberg, P. Chan, R. Mayeux*, et al.*, "Parkinson disease in twins: an etiologic study," *Jama,* vol. 281, pp. 341-346, 1999.
[20] C. Schiesling, N. Kieper, K. Seidel, and R. Krüger, "Familial Parkinson's disease–genetics, clinical phenotype and neuropathology in relation to the common sporadic form of the disease," *Neuropathology and applied neurobiology,* vol. 34, pp. 255-271, 2008.
[21] K. Nuytemans, J. Theuns, M. Cruts, and C. Van Broeckhoven, "Genetic etiology of Parkinson disease associated with mutations in the SNCA, PARK2, PINK1, PARK7, and LRRK2 genes: a mutation update," *Human mutation,* vol. 31, pp. 763-780, 2010.
[22] A. Wood-Kaczmar, S. Gandhi, and N. Wood, "Understanding the molecular causes of Parkinson's disease," *Trends in molecular medicine,* vol. 12, pp. 521-528, 2006.
[23] S. A. Gibson, G.-D. Gao, K. McDonagh, and S. Shen, "Progress on stem cell research towards the treatment of Parkinson's disease," *Stem cell research & therapy,* vol. 3, p. 11, 2012.
[24] S.-L. Ang, "Transcriptional control of midbrain dopaminergic neuron development," *Development,* vol. 133, pp. 3499-3506, 2006.
[25] R. L. Doty, "Olfactory dysfunction in Parkinson disease," *Nature Reviews Neurology,* vol. 8, p. 329, 2012.
[26] P. Limousin, P. Pollak, A. Benazzouz, D. Hoffmann, J.-F. Le Bas, J. E. Perret*, et al.*, "Effect on parkinsonian signs and symptoms of bilateral subthalamic nucleus stimulation," *The Lancet,* vol. 345, pp. 91-95, 1995.
[27] C. W. Olanow, R. L. Watts, and W. C. Koller, "An algorithm (decision tree) for the management of Parkinson's disease (2001): treatment guidelines," *Neurology,* vol. 56, pp. S1-S88, 2001.
[28] A. H. Taub, R. Hogri, A. Magal, M. Mintz, and Y. Shacham-Diamand, "Bioactive anti-inflammatory coating for chronic neural electrodes," *Journal of biomedical materials research Part A,* vol. 100, pp. 1854-1858, 2012.
[29] W. He and R. V. Bellamkonda, "Nanoscale neuro-integrative coatings for neural implants," *Biomaterials,* vol. 26, pp. 2983-2990, 2005.
[30] A. Grill, "Diamond-like carbon coatings as biocompatible materials—an overview," *Diamond and related materials,* vol. 12, pp. 166-170, 2003.
[31] N. Nurdin, P. Francois, Y. Mugnier, J. Krumeich, M. Moret, B. Aronsson*, et al.*, "Haemocompatibility evaluation of DLC-and SiC-coated surfaces," *European Cells and Materials,* vol. 5, pp. 17-28, 2003.
[32] M. Braic, M. Balaceanu, V. Braic, A. Vladescu, G. Pavelescu, and M. Albulescu, "Synthesis and characterization of TiN, TiAlN and TiN/TiAlN biocompatible coatings," *Surface and Coatings Technology,* vol. 200, pp. 1014-1017, 2005.
[33] D. S. Kommireddy, A. A. Patel, T. G. Shutava, D. K. Mills, and Y. M. Lvov, "Layer-by-layer assembly of TiO2 nanoparticles for stable hydrophilic biocompatible coatings," *Journal of nanoscience and nanotechnology,* vol. 5, pp. 1081-1087, 2005.
[34] H. Chen, L. Yuan, W. Song, Z. Wu, and D. Li, "Biocompatible polymer materials: role of protein–surface interactions," *Progress in Polymer Science,* vol. 33, pp. 1059-1087, 2008.
[35] W. Khan, M. Kapoor, and N. Kumar, "Covalent attachment of proteins to functionalized polypyrrole-coated metallic surfaces for improved biocompatibility," *Acta Biomaterialia,* vol. 3, pp. 541-549, 7// 2007.

[36] B. Joddar, A. Albayrak, J. Kang, M. Nishihara, H. Abe, and Y. Ito, "Sustained delivery of siRNA from dopamine-coated stainless steel surfaces," *Acta biomaterialia,* vol. 9, pp. 6753-6761, 2013.
[37] S. F. Cogan, A. A. Guzelian, W. F. Agnew, T. G. Yuen, and D. B. McCreery, "Over-pulsing degrades activated iridium oxide films used for intracortical neural stimulation," *Journal of neuroscience methods,* vol. 137, pp. 141-150, 2004.
[38] E. W. Keefer, B. R. Botterman, M. I. Romero, A. F. Rossi, and G. W. Gross, "Carbon nanotube coating improves neuronal recordings," *Nature nanotechnology,* vol. 3, pp. 434-439, 2008.
[39] S. Minnikanti, P. Skeath, and N. Peixoto, "Electrochemical characterization of multi-walled carbon nanotube coated electrodes for biological applications," *Carbon,* vol. 47, pp. 884-893, 2009.
[40] M. R. Abidian and D. C. Martin, "Experimental and theoretical characterization of implantable neural microelectrodes modified with conducting polymer nanotubes," *Biomaterials,* vol. 29, pp. 1273-1283, 2008.
[41] G. Lind, C. E. Linsmeier, J. Thelin, and J. Schouenborg, "Gelatine-embedded electrodes—a novel biocompatible vehicle allowing implantation of highly flexible microelectrodes," *Journal of neural engineering,* vol. 7, p. 046005, 2010.
[42] X. Zeng, J. Chen, X. Deng, Y. Liu, M. S. Rao, J.-L. Cadet*, et al.*, "An in vitro model of human dopaminergic neurons derived from embryonic stem cells: MPP+ toxicity and GDNF neuroprotection," *Neuropsychopharmacology,* vol. 31, p. 2708, 2006.
[43] B. Xiao, H. H. Ng, R. Takahashi, and E.-K. Tan, "Induced pluripotent stem cells in Parkinson's disease: scientific and clinical challenges," *J Neurol Neurosurg Psychiatry,* pp. jnnp-2015-312036, 2016.
[44] M. J. Devine, M. Ryten, P. Vodicka, A. J. Thomson, T. Burdon, H. Houlden*, et al.*, "Parkinson's disease induced pluripotent stem cells with triplication of the α-synuclein locus," *Nature communications,* vol. 2, p. 440, 2011.
[45] J. Gimsa, B. Habel, U. Schreiber, U. van Rienen, U. Strauss, and U. Gimsa, "Choosing electrodes for deep brain stimulation experiments–electrochemical considerations," *Journal of neuroscience methods,* vol. 142, pp. 251-265, 2005.
[46] G. Manivasagam, D. Dhinasekaran, and A. Rajamanickam, "Biomedical implants: Corrosion and its prevention-a review," *Recent Patents on Corrosion Science,* vol. 2, pp. 40-54, 2010.
[47] M. H. Selim and R. R. Ratan, "The role of iron neurotoxicity in ischemic stroke," *Ageing Research Reviews,* vol. 3, pp. 345-353, 7// 2004.
[48] T. Yoshioka, K. Tsuru, S. Hayakawa, and A. Osaka, "Preparation of alginic acid layers on stainless-steel substrates for biomedical applications," *Biomaterials,* vol. 24, pp. 2889-2894, 2003.
[49] O. Akhavan and E. Ghaderi, "Differentiation of human neural stem cells into neural networks on graphene nanogrids," *Journal of Materials Chemistry B,* vol. 1, pp. 6291-6301, 2013.
[50] Y. Chang, S.-T. Yang, J.-H. Liu, E. Dong, Y. Wang, A. Cao*, et al.*, "In vitro toxicity evaluation of graphene oxide on A549 cells," *Toxicology letters,* vol. 200, pp. 201-210, 2011.

[51] M. Lv, Y. Zhang, L. Liang, M. Wei, W. Hu, X. Li*, et al.*, "Effect of graphene oxide on undifferentiated and retinoic acid-differentiated SH-SY5Y cells line," *Nanoscale,* vol. 4, pp. 3861-3866, 2012.
[52] D. Depan, T. Pesacreta, and R. Misra, "The synergistic effect of a hybrid graphene oxide–chitosan system and biomimetic mineralization on osteoblast functions," *Biomaterials Science,* vol. 2, pp. 264-274, 2014.
[53] S. W. Crowder, D. Prasai, R. Rath, D. A. Balikov, H. Bae, K. I. Bolotin*, et al.*, "Three-dimensional graphene foams promote osteogenic differentiation of human mesenchymal stem cells," *Nanoscale,* vol. 5, pp. 4171-4176, 2013.
[54] Y. Su, V. Kravets, S. Wong, J. Waters, A. Geim, and R. Nair, "Impermeable barrier films and protective coatings based on reduced graphene oxide," *Nature communications,* vol. 5, p. 4843, 09/11/online 2014.
[55] S. K. Singh, M. K. Singh, P. P. Kulkarni, V. K. Sonkar, J. J. Grácio, and D. Dash, "Amine-modified graphene: thrombo-protective safer alternative to graphene oxide for biomedical applications," *Acs Nano,* vol. 6, pp. 2731-2740, 2012.
[56] K. J. Gilmore, G. G. Wallace, H. Chen, M. B. Muller, and D. Li, "Mechanically strong, electrically conductive, and biocompatible graphene," *Advanced materials,* vol. 20, pp. 3557–3561, 2008.
[57] I. K. Moon, J. I. Kim, H. Lee, K. Hur, W. C. Kim, and H. Lee, "2D graphene oxide nanosheets as an adhesive over-coating layer for flexible transparent conductive electrodes," *Scientific reports,* vol. 3, p. 1112, 01/23/online 2013.
[58] K. A. Trzaska and P. Rameshwar, "Dopaminergic neuronal differentiation protocol for human mesenchymal stem cells," *Mesenchymal Stem Cell Assays and Applications,* pp. 295-303, 2011.
[59] N. Tasnim, A. Kumar, and B. Joddar, "Attenuation of the in vitro neurotoxicity of 316L SS by graphene oxide surface coating," *Materials Science and Engineering: C,* 2017.
[60] T. Bouzid, A. Sinitskii, and J. Y. Lim, "Graphene platform for neural regenerative medicine," *Neural regeneration research,* vol. 11, p. 894, 2016.
[61] H. G. Sundararaghavan, G. A. Monteiro, N. A. Lapin, Y. J. Chabal, J. R. Miksan, and D. I. Shreiber, "Genipin-induced changes in collagen gels: Correlation of mechanical properties to fluorescence," *Journal of biomedical materials research Part A,* vol. 87, pp. 308-320, 2008.
[62] C. Hammond, H. Bergman, and P. Brown, "Pathological synchronization in Parkinson's disease: networks, models and treatments," *Trends in neurosciences,* vol. 30, pp. 357-364, 2007.
[63] O. Rascol, P. Payoux, F. Ory, J. J. Ferreira, C. Brefel-Courbon, and J. L. Montastruc, "Limitations of current Parkinson's disease therapy," *Annals of neurology,* vol. 53, 2003.
[64] N. Tasnim, A. Ajam, R. Ramos, M. K. Koripalli, M. Chennamsetti, and Y. Choi, "Handcrafted Electrocorticography Electrodes for a Rodent Behavioral Model," *Technologies,* vol. 4, p. 23, 2016.
[65] T. J. Oxley, N. L. Opie, S. E. John, G. S. Rind, S. M. Ronayne, T. L. Wheeler*, et al.*, "Minimally invasive endovascular stent-electrode array for high-fidelity, chronic recordings of cortical neural activity," *Nature biotechnology,* vol. 34, p. 320, 2016.
[66] P. E. Holtzheimer, M. M. Husain, S. H. Lisanby, S. F. Taylor, L. A. Whitworth, S. McClintock*, et al.*, "Subcallosal cingulate deep brain stimulation for treatment-resistant

depression: a multisite, randomised, sham-controlled trial," *The Lancet Psychiatry,* vol. 4, pp. 839-849, 2017.
[67] A. L. Benabid, "Deep brain stimulation for Parkinson's disease," *Current opinion in neurobiology,* vol. 13, pp. 696-706, 2003.
[68] C. B. Gumera, *New materials and scaffold fabrication method for nerve tissue engineering*: Georgia Institute of Technology, 2009.
[69] D. Szarowski, M. Andersen, S. Retterer, A. Spence, M. Isaacson, H. Craighead*, et al.*, "Brain responses to micro-machined silicon devices," *Brain research,* vol. 983, pp. 23-35, 2003.
[70] G. Decher and J. D. Hong, "Buildup of ultrathin multilayer films by a self-assembly process, 1 consecutive adsorption of anionic and cationic bipolar amphiphiles on charged surfaces," in *Macromolecular Symposia*, 1991, pp. 321-327.
[71] N. Jessel, F. Atalar, P. Lavalle, J. Mutterer, G. Decher, P. Schaaf*, et al.*, "Bioactive coatings based on a polyelectrolyte multilayer architecture functionalized by embedded proteins," *Advanced Materials,* vol. 15, pp. 692-695, 2003.
[72] P. Heiduschka, I. Romann, H. Ecken, M. Schöning, W. Schuhmann, and S. Thanos, "Defined adhesion and growth of neurones on artificial structured substrates," *Electrochimica acta,* vol. 47, pp. 299-307, 2001.
[73] E. Mynttinen, "Differentiation of Human Mesenchymal Stem Cells into Dopaminergic Neurons on Brain Electrode Materials," 2016.
[74] E. K. Purcell, Y. Naim, A. Yang, M. K. Leach, J. M. Velkey, R. K. Duncan*, et al.*, "Combining topographical and genetic cues to promote neuronal fate specification in stem cells," *Biomacromolecules,* vol. 13, pp. 3427-3438, 2012.
[75] A. Gugliandolo, P. Bramanti, and E. Mazzon, "Mesenchymal stem cell therapy in Parkinson's disease animal models," *Current research in translational medicine,* vol. 65, pp. 51-60, 2017.
[76] M. P. Prabhakaran, J. R. Venugopal, and S. Ramakrishna, "Mesenchymal stem cell differentiation to neuronal cells on electrospun nanofibrous substrates for nerve tissue engineering," *Biomaterials,* vol. 30, pp. 4996-5003, 2009.
[77] N. Joyce, G. Annett, L. Wirthlin, S. Olson, G. Bauer, and J. A. Nolta, "Mesenchymal stem cells for the treatment of neurodegenerative disease," *Regenerative medicine,* vol. 5, pp. 933-946, 2010.
[78] J. Arulmoli, "Scaffolds for Neural Stem Cell Tissue Engineering," UC Irvine, 2016.
[79] N. Li, Q. Zhang, S. Gao, Q. Song, R. Huang, L. Wang*, et al.*, "Three-dimensional graphene foam as a biocompatible and conductive scaffold for neural stem cells," *Scientific reports,* vol. 3, p. 1604, 2013.
[80] E. Bressan, L. Ferroni, C. Gardin, L. Sbricoli, L. Gobbato, F. S. Ludovichetti*, et al.*, "Graphene based scaffolds effects on stem cells commitment," *Journal of translational medicine,* vol. 12, p. 296, 2014.
[81] O. Akhavan and E. Ghaderi, "Flash photo stimulation of human neural stem cells on graphene/TiO 2 heterojunction for differentiation into neurons," *Nanoscale,* vol. 5, pp. 10316-10326, 2013.
[82] D. Yang, T. Li, M. Xu, F. Gao, J. Yang, Z. Yang*, et al.*, "Graphene oxide promotes the differentiation of mouse embryonic stem cells to dopamine neurons," *Nanomedicine,* vol. 9, pp. 2445-2455, 2014.

[83] M. Itoh, N. Umegaki-Arao, Z. Guo, L. Liu, C. A. Higgins, and A. M. Christiano, "Generation of 3D skin equivalents fully reconstituted from human induced pluripotent stem cells (iPSCs)," *PloS one,* vol. 8, p. e77673, 2013.
[84] S. Y. Park, J. Park, S. H. Sim, M. G. Sung, K. S. Kim, B. H. Hong*, et al.*, "Enhanced differentiation of human neural stem cells into neurons on graphene," *Advanced Materials,* vol. 23, 2011.
[85] M. Tang, Q. Song, N. Li, Z. Jiang, R. Huang, and G. Cheng, "Enhancement of electrical signaling in neural networks on graphene films," *Biomaterials,* vol. 34, pp. 6402-6411, 2013.
[86] Y. Wang, W. C. Lee, K. K. Manga, P. K. Ang, J. Lu, Y. P. Liu*, et al.*, "Fluorinated Graphene for Promoting Neuro-Induction of Stem Cells," *Advanced Materials,* vol. 24, pp. 4285-4290, 2012.
[87] B. G. Choi, M. Yang, W. H. Hong, J. W. Choi, and Y. S. Huh, "3D macroporous graphene frameworks for supercapacitors with high energy and power densities," *ACS nano,* vol. 6, pp. 4020-4028, 2012.
[88] P. M. Mendes, "Cellular nanotechnology: making biological interfaces smarter," *Chemical Society Reviews,* vol. 42, pp. 9207-9218, 2013.
[89] N. Dubey, R. Bentini, I. Islam, T. Cao, A. H. Castro Neto, and V. Rosa, "Graphene: a versatile carbon-based material for bone tissue engineering," *Stem cells international,* vol. 2015, 2015.
[90] L. Feng and Z. Liu, "Graphene in biomedicine: opportunities and challenges," *Nanomedicine,* vol. 6, pp. 317-324, 2011.
[91] C. Cha, S. R. Shin, N. Annabi, M. R. Dokmeci, and A. Khademhosseini, "Carbon-based nanomaterials: multifunctional materials for biomedical engineering," *ACS nano,* vol. 7, pp. 2891-2897, 2013.
[92] S. Hu, Y. Zeng, S. Yang, H. Qin, H. Cai, and J. Wang, "Application of graphene based nanotechnology in stem cells research," *Journal of nanoscience and nanotechnology,* vol. 15, pp. 6327-6341, 2015.
[93] C. Gardin, A. Piattelli, and B. Zavan, "Graphene in regenerative medicine: focus on stem cells and neuronal differentiation," *Trends in biotechnology,* vol. 34, pp. 435-437, 2016.
[94] K. G. Shah, V. M. Tolosa, A. C. Tooker, S. H. Felix, and S. S. Pannu, "Improved chronic neural stimulation using high surface area platinum electrodes," in *2013 35th Annual International Conference of the IEEE Engineering in Medicine and Biology Society (EMBC)*, Osaka, Japan, 2013, pp. 1546-1549.
[95] D. Depan and R. Misra, "The development, characterization, and cellular response of a novel electroactive nanostructured composite for electrical stimulation of neural cells," *Biomaterials Science,* vol. 2, pp. 1727-1739, 2014.
[96] N. Han, S. S. Rao, J. Johnson, K. S. Parikh, P. A. Bradley, J. J. Lannutti*, et al.*, "Hydrogel–electrospun fiber mat composite coatings for neural prostheses," *Frontiers in neuroengineering,* vol. 4, p. 8, 2011.
[97] G. C. McConnell, H. D. Rees, A. I. Levey, C.-A. Gutekunst, R. E. Gross, and R. V. Bellamkonda, "Implanted neural electrodes cause chronic, local inflammation that is correlated with local neurodegeneration," *Journal of neural engineering,* vol. 6, p. 056003, 2009.

[98] A. M. Jastrzębska, P. Kurtycz, and A. R. Olszyna, "Recent advances in graphene family materials toxicity investigations," *Journal of Nanoparticle Research,* vol. 14, p. 1320, 2012.
[99] Y. Zhu, S. Murali, W. Cai, X. Li, J. W. Suk, J. R. Potts*, et al.*, "Graphene and graphene oxide: synthesis, properties, and applications," *Advanced materials,* vol. 22, pp. 3906-3924, 2010.
[100] S.-R. Ryoo, Y.-K. Kim, M.-H. Kim, and D.-H. Min, "Behaviors of NIH-3T3 fibroblasts on graphene/carbon nanotubes: proliferation, focal adhesion, and gene transfection studies," *Acs Nano,* vol. 4, pp. 6587-6598, 2010.
[101] O. N. Ruiz, K. S. Fernando, B. Wang, N. A. Brown, P. G. Luo, N. D. McNamara*, et al.*, "Graphene oxide: a nonspecific enhancer of cellular growth," *ACS nano,* vol. 5, pp. 8100-8107, 2011.
[102] C. H. Lu, H. H. Yang, C. L. Zhu, X. Chen, and G. N. Chen, "A graphene platform for sensing biomolecules," *Angewandte Chemie,* vol. 121, pp. 4879-4881, 2009.
[103] J. Kim, K. S. Choi, Y. Kim, K. T. Lim, H. Seonwoo, Y. Park*, et al.*, "Bioactive effects of graphene oxide cell culture substratum on structure and function of human adipose-derived stem cells," *Journal of Biomedical Materials Research Part A,* vol. 101, pp. 3520-3530, 2013.
[104] C. Chung, Y.-K. Kim, D. Shin, S.-R. Ryoo, B. H. Hong, and D.-H. Min, "Biomedical applications of graphene and graphene oxide," *Accounts of chemical research,* vol. 46, pp. 2211-2224, 2013.
[105] B. P. O. Alexandra Alcántara Guardado, M.A.I. Shuvo, Yirong Lin , Deidra Hodges, Binata Joddar, "Novel Graphene Oxide biocompatible coatings on 316L Stainless Steel meshes for vascular stent applications," in *BMES*, Tampa, Florida, 2015.
[106] J. Chen, B. Yao, C. Li, and G. Shi, "An improved Hummers method for eco-friendly synthesis of graphene oxide," *Carbon,* vol. 64, pp. 225-229, 2013.
[107] R. Pal, T. O. Monroe, M. Palmieri, M. Sardiello, and G. G. Rodney, "Rotenone induces neurotoxicity through Rac1-dependent activation of NADPH oxidase in SHSY-5Y cells," *FEBS letters,* vol. 588, pp. 472-481, 2014.
[108] M. Li, Q. Liu, Z. Jia, X. Xu, Y. Cheng, Y. Zheng*, et al.*, "Graphene oxide/hydroxyapatite composite coatings fabricated by electrophoretic nanotechnology for biological applications," *Carbon,* vol. 67, pp. 185-197, 2014.
[109] J. Song, X. Wang, and C.-T. Chang, "Preparation and Characterization of Graphene Oxide," *Journal of Nanomaterials,* vol. 2014, p. 6, 2014.
[110] D. C. Marcano, D. V. Kosynkin, J. M. Berlin, A. Sinitskii, Z. Sun, A. Slesarev*, et al.*, "Improved synthesis of graphene oxide," *ACS nano,* vol. 4, pp. 4806-4814, 2010.
[111] G. Lawrie, I. Keen, B. Drew, A. Chandler-Temple, L. Rintoul, P. Fredericks*, et al.*, "Interactions between alginate and chitosan biopolymers characterized using FTIR and XPS," *Biomacromolecules,* vol. 8, pp. 2533-2541, 2007.
[112] G. T. Hermanson, *Bioconjugate techniques*: Academic press, 2013.
[113] D. Beegan, S. Chowdhury, and M. T. Laugier, "Work of indentation methods for determining copper film hardness," *Surface and Coatings Technology,* vol. 192, pp. 57-63, 2005.
[114] W. C. Oliver and G. M. Pharr, "An improved technique for determining hardness and elastic modulus using load and displacement sensing indentation experiments " *Journal of Materials Research,* vol. 7, pp. 1564-1583, 1992.

[115] W. C. Oliver and G. M. Pharr, "Measurment of hardness and elastic modulus by instrumented indentation: Advances in understanding and refinements to methodology," *Journal of Materials Research,* vol. 19, pp. 3-20, 2004.
[116] C. Lee, X. Wei, J. W. Kysar, and J. Hone, "Measurement of the elastic properties and intrinsic strength of monolayer graphene," *Science,* vol. 321, pp. 385-388, 2008.
[117] J. Malzbender, J. M. J. Den Toonder, A. R. Balkenende, and G. De With, "Measuring mechanical properties of coatings: a methodology applied to nano-particle-filled sol–gel coatings on glass," *Materials Science and Engineering: R: Reports,* vol. 36, pp. 47-103, 2002.
[118] B. Joddar, E. Garcia, A. Casas, and C. M. Stewart, "Development of functionalized multi-walled carbon-nanotube-based alginate hydrogels for enabling biomimetic technologies.," *Scientific Reports,* vol. 6, p. 32456, 2016.
[119] S. Ibrahim, B. Joddar, M. Craps, and A. Ramamurthi, "A surface-tethered model to assess size-specific effects of hyaluronan (HA) on endothelial cells," *Biomaterials,* vol. 28, pp. 825-835, 2007.
[120] B. Joddar, M. S. Firstenberg, R. K. Reen, S. Varadharaj, M. Khan, R. C. Childers*, et al.*, "Arterial levels of oxygen stimulate intimal hyperplasia in human saphenous veins via a ROS-dependent mechanism," *PloS one,* vol. 10, p. e0120301, 2015.
[121] J. Taha-Tijerina, D. Venkataramani, C. P. Aichele, C. S. Tiwary, J. E. Smay, A. Mathkar*, et al.*, "Quantification of the Particle Size and Stability of Graphene Oxide in a Variety of Solvents," *Particle & Particle Systems Characterization,* vol. 32, pp. 334-339, 2015.
[122] Y. Han, D. Mayer, A. Offenhäusser, and S. Ingebrandt, "Surface activation of thin silicon oxides by wet cleaning and silanization," *Thin Solid Films,* vol. 510, pp. 175-180, 2006.
[123] M. A. I. Shuvo, M. A. R. Khan, H. Karim, P. Morton, T. Wilson, and Y. Lin, "Investigation of modified graphene for energy storage applications," *ACS applied materials & interfaces,* vol. 5, pp. 7881-7885, 2013.
[124] M. A. I. Shuvo, G. Rodriguez, M. T. Islam, H. Karim, N. Ramabadran, J. C. Noveron*, et al.*, "Microwave Exfoliated Graphene Oxide/TiO2 Nanowire Hybrid for High Performance Lithium Ion Battery," *Journal of Applied Physics,* vol. 118, p. 6, 2015.
[125] Y. Lin, G. J. Ehlert, C. Bukowsky, and H. A. Sodano, "Superhydrophobic Functionalized Graphene Aerogels," *ACS Applied Materials & Interfaces,* vol. 3, pp. 2200-2203, 2011/07/27 2011.
[126] S. R. Meyers and M. W. Grinstaff, "Biocompatible and bioactive surface modifications for prolonged in vivo efficacy," *Chemical reviews,* vol. 112, pp. 1615-1632, 2011.
[127] A. Dey, A. K. Mukhopadhyay, S. Gangadharan, M. K. Sinha, D. Basu, and N. R. Bandyopadhyay, "Nanoindentation study of microplasma sprayed hydroxyapatite coating," *Ceramics International,* vol. 35, pp. 2295-2304, 2009.
[128] K. Alok, B. Krishanu, and B. Bikramjit, "Fretting wear behaviour of hydroxyapatite–titanium composites in simulated body fluid, supplemented with 5 g l −1 bovine serum albumin," *Journal of Physics D: Applied Physics,* vol. 46, p. 404004, 2013.
[129] Q.-Y. Zhang, Y.-Y. Zhang, J. Xie, C.-X. Li, W.-Y. Chen, B.-L. Liu*, et al.*, "Stiff substrates enhance cultured neuronal network activity," *Scientific reports,* vol. 4, p. 6215, 2014.
[130] P. Bianco and P. G. Robey, "Stem cells in tissue engineering," *Nature,* vol. 414, p. 118, 2001.

[131] A. Fabbro, D. Scaini, V. n. León, E. Vázquez, G. Cellot, G. Privitera*, et al.*, "Graphene-based interfaces do not alter target nerve cells," *ACS nano,* vol. 10, pp. 615-623, 2016.
[132] S. J. Chinta and J. K. Andersen, "Dopaminergic neurons," *The international journal of biochemistry & cell biology,* vol. 37, pp. 942-946, 2005.
[133] N. Forraz, K. Wright, M. Jurga, and C. McGuckin, "Experimental therapies for repair of the central nervous system: stem cells and tissue engineering," *Journal of tissue engineering and regenerative medicine,* vol. 7, pp. 523-536, 2013.
[134] C. E. Schmidt and J. B. Leach, "Neural tissue engineering: strategies for repair and regeneration," *Annual review of biomedical engineering,* vol. 5, pp. 293-347, 2003.
[135] G. Bouchez, L. Sensebé, P. Vourc'h, L. Garreau, S. Bodard, A. Rico*, et al.*, "Partial recovery of dopaminergic pathway after graft of adult mesenchymal stem cells in a rat model of Parkinson's disease," *Neurochemistry international,* vol. 52, pp. 1332-1342, 2008.
[136] Y. Wang, J. Yang, H. Li, X. Wang, L. Zhu, M. Fan*, et al.*, "Hypoxia promotes dopaminergic differentiation of mesenchymal stem cells and shows benefits for transplantation in a rat model of Parkinson's disease," *PLoS One,* vol. 8, p. e54296, 2013.
[137] D. Chen, W. Fu, W. Zhuang, C. Lv, F. Li, and X. Wang, "Therapeutic effects of intranigral transplantation of mesenchymal stem cells in rat models of Parkinson's disease," *Journal of neuroscience research,* vol. 95, pp. 907-917, 2017.
[138] F. Wang, T. Yasuhara, T. Shingo, M. Kameda, N. Tajiri, W. J. Yuan*, et al.*, "Intravenous administration of mesenchymal stem cells exerts therapeutic effects on parkinsonian model of rats: focusing on neuroprotective effects of stromal cell-derived factor-1α," *BMC neuroscience,* vol. 11, p. 52, 2010.
[139] B.-N. Park, J.-H. Kim, K. Lee, S. H. Park, and Y.-S. An, "Improved dopamine transporter binding activity after bone marrow mesenchymal stem cell transplantation in a rat model of Parkinson's disease: small animal positron emission tomography study with F-18 FP-CIT," *European radiology,* vol. 25, pp. 1487-1496, 2015.
[140] O. Sadan, M. Bahat-Stromza, Y. Barhum, Y. S. Levy, A. Pisnevsky, H. Peretz*, et al.*, "Protective Effects of Neurotrophic Factor–Secreting Cells in a 6-OHDA Rat Model of Parkinson Disease," *Stem cells and development,* vol. 18, pp. 1179-1190, 2009.
[141] Y. Levy, M. Bahat-Stroomza, R. Barzilay, A. Burshtein, S. Bulvik, Y. Barhum*, et al.*, "Regenerative effect of neural-induced human mesenchymal stromal cells in rat models of Parkinson's disease," *Cytotherapy,* vol. 10, pp. 340-352, 2008.
[142] S. Suzuki, J. Kawamata, N. Iwahara, A. Matsumura, S. Hisahara, T. Matsushita*, et al.*, "Intravenous mesenchymal stem cell administration exhibits therapeutic effects against 6-hydroxydopamine-induced dopaminergic neurodegeneration and glial activation in rats," *Neuroscience letters,* vol. 584, pp. 276-281, 2015.
[143] P. Shetty, G. Ravindran, S. Sarang, A. M. Thakur, H. S. Rao, and C. Viswanathan, "Clinical grade mesenchymal stem cells transdifferentiated under xenofree conditions alleviates motor deficiencies in a rat model of Parkinson's disease," *Cell biology international,* vol. 33, pp. 830-838, 2009.
[144] L. Danielyan, R. Schäfer, A. von Ameln-Mayerhofer, F. Bernhard, S. Verleysdonk, M. Buadze*, et al.*, "Therapeutic efficacy of intranasally delivered mesenchymal stem cells in a rat model of Parkinson disease," *Rejuvenation research,* vol. 14, pp. 3-16, 2011.
[145] N. Xiong, H. Yang, L. Liu, J. Xiong, Z. Zhang, X. Zhang*, et al.*, "bFGF promotes the differentiation and effectiveness of human bone marrow mesenchymal stem cells in a

rotenone model for Parkinson's disease," *Environmental toxicology and pharmacology,* vol. 36, pp. 411-422, 2013.
[146] H. J. Park, P. H. Lee, O. Y. Bang, G. Lee, and Y. H. Ahn, "Mesenchymal stem cells therapy exerts neuroprotection in a progressive animal model of Parkinson's disease," *Journal of neurochemistry,* vol. 107, pp. 141-151, 2008.
[147] Y. J. Kim, H. J. Park, G. Lee, O. Y. Bang, Y. H. Ahn, E. Joe*, et al.*, "Neuroprotective effects of human mesenchymal stem cells on dopaminergic neurons through anti-inflammatory action," *Glia,* vol. 57, pp. 13-23, 2009.
[148] M. L. Khoo, H. Tao, A. C. Meedeniya, A. Mackay-Sim, and D. D. Ma, "Transplantation of neuronal-primed human bone marrow mesenchymal stem cells in hemiparkinsonian rodents," *PLoS One,* vol. 6, p. e19025, 2011.
[149] S. Cerri, R. Greco, G. Levandis, C. Ghezzi, A. S. Mangione, M.-T. Fuzzati-Armentero*, et al.*, "Intracarotid infusion of mesenchymal stem cells in an animal model of parkinson's disease, focusing on cell distribution and neuroprotective and behavioral effects," *Stem cells translational medicine,* vol. 4, pp. 1073-1085, 2015.
[150] D. M. Camp, D. A. Loeffler, D. M. Farrah, J. N. Borneman, and P. A. LeWitt, "Cellular immune response to intrastriatally implanted allogeneic bone marrow stromal cells in a rat model of Parkinson's disease," *Journal of neuroinflammation,* vol. 6, p. 17, 2009.
[151] C. S. Capitelli, C. S. Lopes, A. C. Alves, J. Barbiero, L. F. Oliveira, V. J. D. da Silva*, et al.*, "Opposite effects of bone marrow-derived cells transplantation in MPTP-rat model of Parkinson's disease: a comparison study of mononuclear and mesenchymal stem cells," *International journal of medical sciences,* vol. 11, p. 1049, 2014.
[152] T. Hayashi, S. Wakao, M. Kitada, T. Ose, H. Watabe, Y. Kuroda*, et al.*, "Autologous mesenchymal stem cell–derived dopaminergic neurons function in parkinsonian macaques," *The Journal of clinical investigation,* vol. 123, pp. 272-284, 2013.
[153] N. Zippel, M. Schulze, and E. Tobiasch, "Biomaterials and mesenchymal stem cells for regenerative medicine," *Recent patents on biotechnology,* vol. 4, pp. 1-22, 2010.
[154] E. Krueger, A. N. Chang, D. Brown, J. Eixenberger, R. Brown, S. Rastegar*, et al.*, "Graphene foam as a three-dimensional platform for myotube growth," *ACS biomaterials science & engineering,* vol. 2, pp. 1234-1241, 2016.
[155] J. Sha, C. Gao, S.-K. Lee, Y. Li, N. Zhao, and J. M. Tour, "Preparation of three-dimensional graphene foams using powder metallurgy templates," *ACS nano,* vol. 10, pp. 1411-1416, 2015.
[156] S. M. Willerth, K. J. Arendas, D. I. Gottlieb, and S. E. Sakiyama-Elbert, "Optimization of fibrin scaffolds for differentiation of murine embryonic stem cells into neural lineage cells," *Biomaterials,* vol. 27, pp. 5990-6003, 2006/12/01/ 2006.
[157] K. J. Cho, K. A. Trzaska, S. J. Greco, J. McArdle, F. S. Wang, J. H. Ye*, et al.*, "Neurons derived from human mesenchymal stem cells show synaptic transmission and can be induced to produce the neurotransmitter substance P by interleukin-1α," *Stem cells,* vol. 23, pp. 383-391, 2005.
[158] K. J. Brennand, M. C. Marchetto, N. Benvenisty, O. Brüstle, A. Ebert, J. C. I. Belmonte*, et al.*, "Creating patient-specific neural cells for the in vitro study of brain disorders," *Stem cell reports,* vol. 5, pp. 933-945, 2015.
[159] J. E. Beevers, T. M. Caffrey, and R. Wade-Martins, "Induced pluripotent stem cell (iPSC)-derived dopaminergic models of Parkinson's disease," *Biochemical Society Transactions,* vol. 41, pp. 1503-1508, 2013.

[160] J. Candy, R. Perry, E. Perry, D. Irving, G. Blessed, A. Fairbairn*, et al.*, "Pathological changes in the nucleus of Meynert in Alzheimer's and Parkinson's diseases," *Journal of the neurological sciences,* vol. 59, pp. 277-289, 1983.
[161] J.-H. Kim, J. M. Auerbach, J. A. Rodríguez-Gómez, I. Velasco, D. Gavin, N. Lumelsky*, et al.*, "Dopamine neurons derived from embryonic stem cells function in an animal model of Parkinson's disease," *Nature,* vol. 418, pp. 50-56, 2002.
[162] O. Lindvall and A. Björklund, "Cell therapy in Parkinson's disease," *NeuroRx,* vol. 1, pp. 382-393, 2004.
[163] O. Lindvall and Z. Kokaia, "Prospects of stem cell therapy for replacing dopamine neurons in Parkinson's disease," *Trends in Pharmacological sciences,* vol. 30, pp. 260-267, 2009.
[164] B. Xiao, H. H. Ng, R. Takahashi, and E.-K. Tan, "Induced pluripotent stem cells in Parkinson's disease: scientific and clinical challenges," *Journal of Neurology, Neurosurgery & Psychiatry,* vol. 87, pp. 697-702, 2016.
[165] P. Soman, B. T. D. Tobe, J. W. Lee, A. M. Winquist, I. Singec, K. S. Vecchio*, et al.*, "Three-dimensional scaffolding to investigate neuronal derivatives of human embryonic stem cells," *Biomedical microdevices,* vol. 14, pp. 829-838, 2012.
[166] M. Tang, Q. Song, N. Li, Z. Jiang, R. Huang, and G. Cheng, "Enhancement of electrical signaling in neural networks on graphene films," *Biomaterials,* vol. 34, pp. 6402-11, Sep 2013.
[167] A. A. John, A. P. Subramanian, M. V. Vellayappan, A. Balaji, H. Mohandas, and S. K. Jaganathan, "Carbon nanotubes and graphene as emerging candidates in neuroregeneration and neurodrug delivery," *Int J Nanomedicine,* vol. 10, pp. 4267-77, 2015.
[168] N. Li, X. Zhang, Q. Song, R. Su, Q. Zhang, T. Kong*, et al.*, "The promotion of neurite sprouting and outgrowth of mouse hippocampal cells in culture by graphene substrates," *Biomaterials,* vol. 32, pp. 9374-82, Dec 2011.
[169] J. Kim, S. Park, Y. J. Kim, C. S. Jeon, K. T. Lim, H. Seonwoo*, et al.*, "Monolayer Graphene-Directed Growth and Neuronal Differentiation of Mesenchymal Stem Cells," *J Biomed Nanotechnol,* vol. 11, pp. 2024-33, Nov 2015.
[170] S. Y. Park, J. Park, S. H. Sim, M. G. Sung, K. S. Kim, B. H. Hong*, et al.*, "Enhanced differentiation of human neural stem cells into neurons on graphene," *Adv Mater,* vol. 23, pp. H263-7, Sep 22 2011.
[171] T. Kim, Y. H. Kahng, T. Lee, K. Lee, and D. H. Kim, "Graphene Films Show Stable Cell Attachment and Biocompatibility with Electrogenic Primary Cardiac Cells," *Molecules and Cells,* vol. 36, pp. 577-582, 11/29
[172] I. Kanayama, H. Miyaji, H. Takita, E. Nishida, M. Tsuji, B. Fugetsu*, et al.*, "Comparative study of bioactivity of collagen scaffolds coated with graphene oxide and reduced graphene oxide," *International Journal of Nanomedicine,* vol. 9, pp. 3363-3373, 07/11 2014.
[173] T. J. Hinton, Q. Jallerat, R. N. Palchesko, J. H. Park, M. S. Grodzicki, H.-J. Shue*, et al.*, "Three-dimensional printing of complex biological structures by freeform reversible embedding of suspended hydrogels," *Science advances,* vol. 1, p. e1500758, 2015.
[174] A. Bigi, G. Cojazzi, S. Panzavolta, N. Roveri, and K. Rubini, "Stabilization of gelatin films by crosslinking with genipin," *Biomaterials,* vol. 23, pp. 4827-4832, 2002.

[175] H. W. Sung, W. H. Chang, C. Y. Ma, and M. H. Lee, "Crosslinking of biological tissues using genipin and/or carbodiimide," *Journal of Biomedical Materials Research Part A,* vol. 64, pp. 427-438, 2003.
[176] R. S. Stowers, S. C. Allen, and L. J. Suggs, "Dynamic phototuning of 3D hydrogel stiffness," *Proceedings of the National Academy of Sciences,* vol. 112, pp. 1953-1958, 2015.
[177] K. A. Trzaska and P. Rameshwar, "Dopaminergic neuronal differentiation protocol for human mesenchymal stem cells," *Methods Mol Biol,* vol. 698, pp. 295-303, 2011.
[178] B. Joddar, A. T. Guy, H. Kamiguchi, and Y. Ito, "Spatial gradients of chemotropic factors from immobilized patterns to guide axonal growth and regeneration," *Biomaterials,* vol. 34, pp. 9593-9601, 2013.
[179] R. Duan, J. Zhang, X. Du, X. Yao, and K. Konno, "Properties of collagen from skin, scale and bone of carp (Cyprinus carpio)," *Food Chemistry,* vol. 112, pp. 702-706, 2009/02/01/ 2009.
[180] H. Y. Yue, S. Huang, J. Chang, C. Heo, F. Yao, S. Adhikari*, et al.*, "ZnO Nanowire Arrays on 3D Hierachical Graphene Foam: Biomarker Detection of Parkinson's Disease," *ACS Nano,* vol. 8, pp. 1639-1646, 2014/02/25 2014.
[181] D. Kumari, L. Sheikh, S. Bhattacharya, T. J. Webster, and S. Nayar, "Two-dimensional collagen-graphene as colloidal templates for biocompatible inorganic nanomaterial synthesis," *Int J Nanomedicine,* vol. 12, pp. 3605-3616, 2017.
[182] R. Deepachitra, V. Ramnath, and T. P. Sastry, "Graphene oxide incorporated collagen-fibrin biofilm as a wound dressing material," *RSC Advances,* vol. 4, pp. 62717-62727, 2014.
[183] S. Huang, H. Yue, J. Zhou, J. Zhang, C. Zhang, X. Gao*, et al.*, "Highly Selective and Sensitive Determination of Dopamine in the Presence of Ascorbic Acid Using a 3D Graphene Foam Electrode," *Electroanalysis,* vol. 26, pp. 184-190, 2014.
[184] Y. Wang, N. Van Manh, H. Wang, X. Zhong, X. Zhang, and C. Li, "Synergistic intrafibrillar/extrafibrillar mineralization of collagen scaffolds based on a biomimetic strategy to promote the regeneration of bone defects," *Int J Nanomedicine,* vol. 11, pp. 2053-67, 2016.
[185] A. Roskams, X. Cai, and G. Ronnett, "Expression of neuron-specific beta-III tubulin during olfactory neurogenesis in the embryonic and adult rat," *Neuroscience,* vol. 83, pp. 191-200, 1998.
[186] A. Weyer and K. Schilling, "Developmental and cell type-specific expression of the neuronal marker NeuN in the murine cerebellum," *Journal of neuroscience research,* vol. 73, pp. 400-409, 2003.
[187] H. Kawasaki, K. Mizuseki, S. Nishikawa, S. Kaneko, Y. Kuwana, S. Nakanishi*, et al.*, "Induction of midbrain dopaminergic neurons from ES cells by stromal cell–derived inducing activity," *neuron,* vol. 28, pp. 31-40, 2000.
[188] K. Takahashi, K. Tanabe, M. Ohnuki, M. Narita, T. Ichisaka, K. Tomoda*, et al.*, "Induction of pluripotent stem cells from adult human fibroblasts by defined factors," *cell,* vol. 131, pp. 861-872, 2007.
[189] J.-M. Peyrin, B. Deleglise, L. Saias, M. Vignes, P. Gougis, S. Magnifico*, et al.*, "Axon diodes for the reconstruction of oriented neuronal networks in microfluidic chambers," *Lab on a Chip,* vol. 11, pp. 3663-3673, 2011.

[190] N. Li, Q. Zhang, S. Gao, Q. Song, R. Huang, L. Wang*, et al.*, "Three-dimensional graphene foam as a biocompatible and conductive scaffold for neural stem cells," *Sci Rep,* vol. 3, p. 1604, 2013.
[191] J. K. Wang, G. M. Xiong, M. Zhu, B. Özyilmaz, A. H. Castro Neto, N. S. Tan*, et al.*, "Polymer-Enriched 3D Graphene Foams for Biomedical Applications," *ACS Applied Materials & Interfaces,* vol. 7, pp. 8275-8283, 2015/04/22 2015.
[192] H. H. Yoon, S. H. Bhang, T. Kim, T. Yu, T. Hyeon, and B. S. Kim, "Dual Roles of Graphene Oxide in Chondrogenic Differentiation of Adult Stem Cells: Cell-Adhesion Substrate and Growth Factor-Delivery Carrier," *Advanced Functional Materials,* vol. 24, pp. 6455-6464, 2014.
[193] F. P. Di Giorgio, M. A. Carrasco, M. C. Siao, T. Maniatis, and K. Eggan, "Non–cell autonomous effect of glia on motor neurons in an embryonic stem cell–based ALS model," *Nature neuroscience,* vol. 10, pp. 608-614, 2007.
[194] J. T. Dimos, K. T. Rodolfa, K. K. Niakan, L. M. Weisenthal, H. Mitsumoto, W. Chung*, et al.*, "Induced pluripotent stem cells generated from patients with ALS can be differentiated into motor neurons," *science,* vol. 321, pp. 1218-1221, 2008.
[195] D. A. Grow, D. V. Simmons, J. A. Gomez, M. J. Wanat, J. R. McCarrey, C. A. Paladini*, et al.*, "Differentiation and Characterization of Dopaminergic Neurons From Baboon Induced Pluripotent Stem Cells," *Stem Cells Translational Medicine,* vol. 5, pp. 1133-1144, 2016.
[196] K. Jong-Hoon, J. M. Auerbach, J. A. Rodríguez-Gómez, and I. Velasco, "Dopamine neurons derived from embryonic stem cells function in an animal model of Parkinson's disease," *Nature,* vol. 418, p. 50, 2002.
[197] S. Karumbayaram, B. G. Novitch, M. Patterson, J. A. Umbach, L. Richter, A. Lindgren*, et al.*, "Directed Differentiation of Human-Induced Pluripotent Stem Cells Generates Active Motor Neurons," *Stem cells,* vol. 27, pp. 806-811, 2009.
[198] K. Oki, J. Tatarishvili, J. Wood, P. Koch, S. Wattananit, Y. Mine*, et al.*, "Human-induced pluripotent stem cells form functional neurons and improve recovery after grafting in stroke-damaged brain," *Stem cells,* vol. 30, pp. 1120-1133, 2012.
[199] A. M. Paşca, S. A. Sloan, L. E. Clarke, Y. Tian, C. D. Makinson, N. Huber*, et al.*, "Functional cortical neurons and astrocytes from human pluripotent stem cells in 3D culture," *Nature methods,* vol. 12, pp. 671-678, 2015.
[200] P. P. Peruzzi, S. E. Lawler, S. L. Senior, N. Dmitrieva, P. A. Edser, D. Gianni*, et al.*, "Physiological transgene regulation and functional complementation of a neurological disease gene deficiency in neurons," *Molecular Therapy,* vol. 17, pp. 1517-1526, 2009.
[201] J. A. Stogsdill and C. Eroglu, "The interplay between neurons and glia in synapse development and plasticity," *Current opinion in neurobiology,* vol. 42, pp. 1-8, 2017.
[202] A. Swistowski, J. Peng, Q. Liu, P. Mali, M. S. Rao, L. Cheng*, et al.*, "Efficient generation of functional dopaminergic neurons from human induced pluripotent stem cells under defined conditions," *Stem cells,* vol. 28, pp. 1893-1904, 2010.
[203] A. Iwanami, S. Kaneko, M. Nakamura, Y. Kanemura, H. Mori, S. Kobayashi*, et al.*, "Transplantation of human neural stem cells for spinal cord injury in primates," *Journal of neuroscience research,* vol. 80, pp. 182-190, 2005.
[204] N. Gardiner and O. Freeman, "Chapter Five-Can Diabetic Neuropathy Be Modeled In Vitro?," *International review of neurobiology,* vol. 127, pp. 53-87, 2016.

[205] H. Craighead, S. Turner, R. Davis, C. James, A. Perez, P. S. John*, et al.*, "Chemical and topographical surface modification for control of central nervous system cell adhesion," *Biomedical Microdevices,* vol. 1, pp. 49-64, 1998.
[206] D. Jgamadze, L. Liu, S. Vogler, L.-Y. Chu, and S. Pautot, "Thermoswitching microgel carriers improve neuronal cell growth and cell release for cell transplantation," *Tissue Engineering Part C: Methods,* vol. 21, pp. 65-76, 2014.
[207] Y. Li, H. Meng, Y. Liu, and B. P. Lee, "Fibrin gel as an injectable biodegradable scaffold and cell carrier for tissue engineering," *The Scientific World Journal,* vol. 2015, 2015.

Vita

Nishat Tasnim was born on January 25, 1991 in Dhaka, Bangladesh. She is the daughter of Mr. Abu Mahmud and Mrs. Afroza Mahmud. She earned her Bachelor's degree in Electrical and Electronic Engineering from Ahsanullah University of Science & Technology, Dhaka, Bangladesh in 2013. She received her Master's degree in Electrical Engineering from The University of Texas Rio Grande Valley (UTRGV) in 2016. In the same year, she joined the Doctoral program in Materials Science & Engineering at The University of Texas at El Paso (UTEP). Nishat worked as a Research Assistant throughout her graduate studies. She received Presidential Graduate Scholarship, Anita Mochen Loya Graduate Engineering Fellowship, College of Engineering Award, Graduate Research Award, and state of Texas Public Education Grant (TPEG) for international students, while pursuing her Master's and Doctoral studies. She participated in several international research symposiums and published several book-chapters and research papers as the first author.

Permanent address: 52/3 South Bashabo,
Dhaka-1214, Bangladesh

This dissertation was typed by Nishat Tasnim.